

# Inflation connected to the origin of CP violation

メタデータ	言語: eng 出版者: 公開日: 2022-01-07 キーワード (Ja): キーワード (En): 作成者: メールアドレス: 所属:
URL	<a href="https://doi.org/10.24517/00064656">https://doi.org/10.24517/00064656</a>

This work is licensed under a Creative Commons Attribution-NonCommercial-ShareAlike 3.0 International License.




## Inflation connected to the origin of $CP$ violation

Tsuyoshi Hashimoto<sup>1,\*</sup>, Norma Sidik Risdianto<sup>1,2,†</sup> and Daijiro Suematsu<sup>1,‡</sup>

<sup>1</sup>*Institute for Theoretical Physics, Kanazawa University, Kanazawa 920-1192, Japan*

<sup>2</sup>*Department of Physics Education, Universitas Islam Negeri Sunan Kalijaga, Jl. Marsda Adisucipto, Yogyakarta 55280, Indonesia*

 (Received 13 May 2021; accepted 1 October 2021; published 27 October 2021)

We consider a simple extension of the standard model, which could give a solution for its  $CP$  issues such as the origin of both Cabibbo-Kobayashi-Maskawa (CKM) and Pontecorvo-Maki-Nakagawa-Sakata (PMNS) phases and the strong  $CP$  problem. The model is extended with singlet scalars which allow the introduction of the Peccei-Quinn symmetry and could cause spontaneous  $CP$  violation to result in these phases at low energy regions. The singlet scalars could give a good inflaton candidate if they have a suitable nonminimal coupling with the Ricci scalar.  $CP$  issues and inflation could be closely related through these singlet scalars in a natural way. In a case where the inflaton is a mixture of the singlet scalars, we study reheating and leptogenesis as notable phenomena affected by the fields introduced in this extension.

DOI: [10.1103/PhysRevD.104.075034](https://doi.org/10.1103/PhysRevD.104.075034)

### I. INTRODUCTION

$CP$  symmetry is a fundamental discrete symmetry that plays an important role in particle physics. In the standard model (SM), it is considered to be violated explicitly through complex Yukawa coupling constants [1] and a  $\theta$  parameter in the QCD sector [2]. The former is known to explain very well  $CP$  violating phenomena in  $B$  meson systems and so on [3]. The latter is severely constrained through an experimental search of a neutron electric dipole moment [4] and causes the notorious strong  $CP$  problem [5]. Peccei-Quinn (PQ) symmetry has been proposed to solve it [6]. If we assume that the  $CP$  symmetry is an original symmetry of nature, the complex phases of Yukawa coupling constants have to be spontaneously induced through some mechanism at high energy regions. It may be compactification dynamics in string theory near at the Planck scale [7]. In that case, since nonzero  $\theta$  could be caused through radiative effects after the  $CP$  violation, the PQ symmetry is required to solve the strong  $CP$  problem again.

As an alternative scenario for the realization of  $CP$  symmetry, we may consider it to be exact so that all coupling constants, including Yukawa couplings, are real

and also that  $\theta$  is kept to some scale much lower than the Planck scale. In that case, the  $CP$  symmetry is supposed to be spontaneously broken, and this violation can be expected to be transformed to a complex phase in the CKM matrix effectively. If nonzero  $\theta$  is not brought about in this process, then it is favorable for the strong  $CP$  problem. The Nelson-Barr (NB) mechanism [8] has been proposed as such a concrete example. Unfortunately, radiative effects could cause a nonzero  $\theta$  with a magnitude that contradicts the experimental constraints [9].<sup>1</sup> However, the scenario is interesting since it can present an explanation for the origin of the  $CP$  violation at a much lower energy region than the Planck scale. As a realization of the NB mechanism, a simple model has been proposed in [10]. The model is extended in [11] to the lepton sector where the existence of a  $CP$  violating phase in the PMNS matrix [12] is suggested through recent neutrino oscillation experiments [13].

Observations of the cosmic microwave background (CMB) fluctuation [14,15] suggest the existence of the exponential expansion of the Universe called “inflation.” Inflation is usually considered to be induced by some slowly rolling scalar field called “inflaton” [16]. It is a crucial problem to identify its candidate from a viewpoint of the extension of the SM. Although the Higgs scalar has been studied as a promising candidate in the SM [17] under an assumption that it has a nonminimal coupling with the Ricci scalar curvature [18], several problems have been pointed out [19–21]. In this situation, it is interesting to find

\*[t\\_hashimoto@hep.s.kanazawa-u.ac.jp](mailto:t_hashimoto@hep.s.kanazawa-u.ac.jp)

†[norma.risdianto@uin-suka.ac.id](mailto:norma.risdianto@uin-suka.ac.id)

‡[suematsu@hep.s.kanazawa-u.ac.jp](mailto:suematsu@hep.s.kanazawa-u.ac.jp)

Published by the American Physical Society under the terms of the [Creative Commons Attribution 4.0 International](https://creativecommons.org/licenses/by/4.0/) license. Further distribution of this work must maintain attribution to the author(s) and the published article’s title, journal citation, and DOI. Funded by SCOAP<sup>3</sup>.

<sup>1</sup>Introduction of the PQ symmetry could solve this fault of the model. We consider such a possibility in the extension of the model.

an alternative candidate for inflaton in a certain extension of the SM that could solve several problems in the SM. In this sense, the model extended from a viewpoint of the  $CP$  symmetry as described above could give such a promising candidate. It contains singlet scalars that cause the spontaneous  $CP$  violation and allow the introduction of the PQ symmetry as a solution for the strong  $CP$  problem. If they couple with the scalar curvature nonminimally, then it could cause slow-roll inflation successfully. In this paper, we discuss such a possibility that the inflation of the Universe could be related to the  $CP$  violation in the SM. We study reheating and leptogenesis as its phenomenology caused by extra fields introduced in the model to solve the  $CP$  issues.

Remaining parts of the paper are organized as follows. In Sec. II, we describe the model studied in this paper and discuss both phases in the CKM and PMNS matrices that are derived as a result of the spontaneous  $CP$  violation. In Sec. III, we discuss the inflation brought about by the singlet scalars which are related to the  $CP$  issues and the reheating. After that, we describe leptogenesis that could show a distinguishable feature from the usual leptogenesis in the seesaw model. The paper is summarized in Sec. IV.

## II. ORIGIN OF $CP$ VIOLATION

### A. An extended model

Our model is an  $CP$  invariant extension of the SM with global  $U(1) \times Z_4$  symmetry and several additional fields. As fermions, we introduce a pair of vectorlike down-type quarks  $(D_L, D_R)$ , a pair of vectorlike charged leptons  $(E_L, E_R)$ , and three right-handed singlet fermions  $N_j$  ( $j = 1, 2, 3$ ).<sup>2</sup> We also introduce an additional doublet scalar  $\eta$  and two singlet complex scalars  $\sigma$  and  $S$ . Their representation and charge under the symmetry  $[SU(3)_C \times SU(2)_L \times U(1)_Y] \times U(1) \times Z_4$  are summarized in Table I.<sup>3</sup> The SM contents are assumed to have no charge of the global symmetry. Since this global  $U(1)$  has a color anomaly in the same way as the Kim-Shifman-Vainstein-Zakharov (KSVZ) model [23] for a strong  $CP$  problem, it can play the role of PQ symmetry. The present charge assignment for colored fermions guarantees the domain wall number to be one ( $N_{DW} = 1$ ) so that the model can escape the domain wall problem [24,25].

The model is characterized by new Yukawa terms and scalar potential, which are invariant under the imposed symmetry

$$\begin{aligned}
-\mathcal{L}_Y &= y_D \sigma \bar{D}_L D_R + y_E \sigma \bar{E}_L E_R + \sum_{j=1}^3 \left( \frac{y_{N_j}}{2} \sigma \bar{N}_j^c N_j + y_{d_j} S \bar{D}_L d_{R_j} + \tilde{y}_{d_j} S^\dagger \bar{D}_L d_{R_j} \right. \\
&\quad \left. + y_{e_j} S \bar{E}_L e_{R_j} + \tilde{y}_{e_j} S^\dagger \bar{E}_L e_{R_j} + \sum_{\alpha=1}^3 h_{\alpha j}^* \eta \bar{\ell}_\alpha N_j \right) + \sum_{\alpha,\beta=1}^3 \frac{y_{\alpha\beta}}{M_*} (\bar{\ell}_\alpha \phi) (\bar{\ell}_\beta \phi) + \text{H.c.}, \\
V &= \lambda_1 (\phi^\dagger \phi)^2 + \lambda_2 (\eta^\dagger \eta)^2 + \lambda_3 (\phi^\dagger \phi) (\eta^\dagger \eta) + \lambda_4 (\phi^\dagger \eta) (\eta^\dagger \phi) + \frac{\lambda_5}{2M_*} [\sigma (\eta^\dagger \phi)^2 + \text{H.c.}] \\
&\quad + \kappa_\sigma (\sigma^\dagger \sigma)^2 + \kappa_S (S^\dagger S)^2 + (\kappa_{\phi\sigma} \phi^\dagger \phi + \kappa_{\eta\sigma} \eta^\dagger \eta) (\sigma^\dagger \sigma) + (\kappa_{\phi S} \phi^\dagger \phi + \kappa_{\eta S} \eta^\dagger \eta) (S^\dagger S) \\
&\quad + \kappa_{\sigma S} (\sigma^\dagger \sigma) (S^\dagger S) + m_\phi^2 \phi^\dagger \phi + m_\eta^2 \eta^\dagger \eta + m_\sigma^2 \sigma^\dagger \sigma + m_S^2 S^\dagger S + V_b,
\end{aligned} \tag{1}$$

where  $d_{R_j}$  and  $e_{R_j}$  are the SM down-type quarks and charged leptons, respectively.  $\ell_\alpha$  is a doublet lepton and  $\phi$  is an ordinary doublet Higgs scalar. Since  $CP$  invariance is assumed, parameters in the Lagrangian are considered to be all real. In Eq. (1), we list dominant terms up to dimension five, and  $M_*$  is a cutoff scale of the model. Other invariant terms are higher order and can be safely neglected in comparison with the listed ones.  $V_b$  is composed of terms that are invariant under the global symmetry but violate the  $S$  number.

For a while, we focus on a part of field space where the field values of  $\sigma$  and  $S$  are much larger than both  $\phi$  and  $\eta$  to

study the potential composed of  $\sigma$  and  $S$  only. In the present study, we assume that  $V_b$  takes a following form<sup>4</sup>:

$$\begin{aligned}
V_b &= \alpha (S^4 + S^{\dagger 4}) + \beta \sigma^\dagger \sigma (S^2 + S^{\dagger 2}) \\
&= \frac{1}{2} \tilde{S}^2 (\alpha \tilde{S}^2 \cos 4\rho + \beta \tilde{\sigma}^2 \cos 2\rho),
\end{aligned} \tag{2}$$

where we define  $\sigma = \frac{\tilde{\sigma}}{\sqrt{2}} e^{i\theta}$  and  $S = \frac{\tilde{S}}{\sqrt{2}} e^{i\rho}$ . Along the minimum of  $V_b$  for  $\rho$ , which is fixed by  $\frac{\partial V_b}{\partial \rho} = 0$ , the potential of  $\tilde{\sigma}$  and  $\tilde{S}$  can be written as

<sup>2</sup>Similar models with vectorlike extra fermions have been considered under different symmetry structures [11,22].

<sup>3</sup> $Z_4$  is imposed by hand to control the couplings of the new fields to the SM contents.

<sup>4</sup>Imposed symmetry allows terms  $m_S^2 (S^2 + S^{\dagger 2})$  in  $V_b$ . However, we assume that their contribution is negligible since we focus our attention on a potential valley where  $\tilde{\sigma} \propto \tilde{S}$  is satisfied, and then  $\cos 2\rho$  could be a constant at the minimum of  $V_b$  in that case.

TABLE I. New fields added to the SM and their representation and charge under  $[SU(3)_C \times SU(2)_L \times U(1)_Y] \times U(1) \times Z_4$ .

	$SU(3)_C$	$SU(2)_L$	$U(1)_Y$	$U(1)$	$Z_4$		$SU(3)_C$	$SU(2)_L$	$U(1)_Y$	$U(1)$	$Z_4$
$D_L$	<b>3</b>	<b>1</b>	$-\frac{1}{3}$	0	2	$D_R$	<b>3</b>	<b>1</b>	$-\frac{1}{3}$	2	0
$E_L$	<b>1</b>	<b>1</b>	-1	0	2	$E_R$	<b>1</b>	<b>1</b>	-1	2	0
$\sigma$	<b>1</b>	<b>1</b>	0	-2	2	$S$	<b>1</b>	<b>1</b>	0	0	2
$N_k$	<b>1</b>	<b>1</b>	0	1	1	$\eta$	<b>1</b>	<b>2</b>	$-\frac{1}{2}$	-1	-1

$$V(\tilde{\sigma}, \tilde{S}) = \frac{\tilde{\kappa}_\sigma}{4} (\tilde{\sigma}^2 - w^2)^2 + \frac{\tilde{\kappa}_S}{4} (\tilde{S}^2 - u^2)^2 + \frac{\kappa_{\sigma S}}{4} (\tilde{\sigma}^2 - w^2)(\tilde{S}^2 - u^2), \quad (3)$$

where  $\tilde{\kappa}_\sigma$  and  $\tilde{\kappa}_S$  are defined as

$$\tilde{\kappa}_\sigma = \kappa_\sigma - \frac{\beta^2}{4\alpha}, \quad \tilde{\kappa}_S = \kappa_S - 2\alpha, \quad (4) \quad \tilde{\kappa}_\sigma, \tilde{\kappa}_S > 0, \quad 4\tilde{\kappa}_\sigma\tilde{\kappa}_S > \kappa_{\sigma S}^2. \quad (5)$$

and  $w$  and  $u$  are the vacuum expectation values (VEVs) of  $\tilde{\sigma}$  and  $\tilde{S}$ . They are supposed to be much larger than the weak scale. They keep the gauge symmetry but break down the global symmetry  $U(1) \times Z_4$  into its diagonal subgroup  $Z_2$ .<sup>5</sup> Since the minimum of  $V_b$  can be determined by using these

VEVs as  $\cos 2\rho = -\frac{\beta w^2}{4\alpha u^2}$  as long as  $|\frac{\beta w^2}{4\alpha u^2}| \leq 1$  is satisfied, the  $CP$  symmetry is spontaneously broken to result in a low energy effective model with the  $CP$  violation. On the other hand,  $\theta = 0$  is satisfied because of the global  $U(1)$  symmetry relevant to  $\sigma$  [26]. The stability condition for the potential (3) can be given as

If we consider the fluctuation of  $\tilde{\sigma}$  and  $\tilde{S}$  around the vacua  $\langle \tilde{\sigma} \rangle$  and  $\langle \tilde{S} \rangle$ , then mass eigenstates are the mixture of them in general. If we take account of the stability condition (5), then mass eigenvalues can be approximately expressed as

$$m_\xi^2 \simeq 2 \left( \tilde{\kappa}_S - \frac{\kappa_{\sigma S}^2}{4\tilde{\kappa}_\sigma} \right) u^2 \equiv 2\hat{\kappa}_S u^2, \quad m_\sigma^2 \simeq 2\tilde{\kappa}_\sigma w^2 \quad \text{for } \tilde{\kappa}_\sigma^2 w^2 \gg \tilde{\kappa}_S^2 u^2, \\ m_\xi^2 \simeq 2\tilde{\kappa}_S u^2, \quad m_\sigma^2 \simeq 2 \left( \tilde{\kappa}_\sigma - \frac{\kappa_{\sigma S}^2}{4\tilde{\kappa}_S} \right) w^2 \equiv 2\hat{\kappa}_\sigma w^2 \quad \text{for } \tilde{\kappa}_S^2 u^2 \gg \tilde{\kappa}_\sigma^2 w^2. \quad (6)$$

Although they have a tiny subcomponent in these cases, a dominant component of their eigenstates is  $\tilde{S}$  and  $\tilde{\sigma}$ , respectively. The mass of an orthogonal component to  $\tilde{S}$  is found to be  $m_{\xi_\perp}^2 = 8\alpha u^2(1 - \cos^2 2\rho)$ . Since the global  $U(1)$  symmetry works as the PQ symmetry mentioned above, and the axion decay constant is given as  $f_a = w$ , the VEV  $w$  should satisfy the following condition [3,27]:

$$4 \times 10^8 \text{ GeV} \lesssim w \lesssim 10^{11} \text{ GeV}. \quad (7)$$

The Nambu-Goldstone (NG) boson caused by the spontaneous breaking of this  $U(1)$  becomes an axion [28] that is characterized by a coupling with photons [29]:

$$g_{a\gamma\gamma} = \frac{1.51}{10^{10} \text{ GeV}} \left( \frac{m_a}{\text{eV}} \right). \quad (8)$$

<sup>5</sup>It guarantees the stability of the lightest  $Z_2$  odd field, which could be a dark matter (DM) candidate as discussed later.

In the next part, we show that the effective model after the symmetry breaking can have  $CP$  phases in the CKM and PMNS matrices. They are induced by the mass matrices for the down type quarks and the charged leptons through a similar mechanism that has been discussed in [10] as a simple realization of the NB mechanism [8] for the strong  $CP$  problem.

## B. $CP$ violating phases in CKM and PMNS matrices

Yukawa couplings of down-type quarks and charged leptons given in Eq. (1) derive mass terms as

$$(\bar{f}_{Li}, \bar{F}_L) \mathcal{M}_f \begin{pmatrix} f_{Rj} \\ F_R \end{pmatrix} + \text{H.c.}, \quad \mathcal{M}_f = \begin{pmatrix} m_{f_{ij}} & 0 \\ \mathcal{F}_{f_j} & \mu_F \end{pmatrix}, \quad (9)$$

where  $f$  and  $F$  represent  $f = d, e$  and  $F = D, E$  for down-type quarks and charged leptons and  $\mathcal{M}_f$  is a  $4 \times 4$  matrix. Each component of  $\mathcal{M}_f$  is expressed as  $m_{f_{ij}} = h_{f_{ij}} \langle \tilde{\phi} \rangle$ ,  $\mathcal{F}_{f_j} = (y_{f_j} u e^{i\rho} + \tilde{y}_{f_j} u e^{-i\rho})$  and  $\mu_F = y_F w$ . This mass matrix is found to have the same form proposed in [10].

Since the global  $U(1)$  symmetry works as the PQ symmetry, and all parameters in the model are assumed to be real,  $\arg(\det \mathcal{M}_f) = 0$  is satisfied even if radiative effects are taken into account after the spontaneous breaking of the  $CP$  symmetry [11].

We consider the diagonalization of a matrix  $\mathcal{M}_f \mathcal{M}_f^\dagger$  by a unitary matrix

$$\begin{pmatrix} A_f & B_f \\ C_f & D_f \end{pmatrix} \begin{pmatrix} m_f m_f^\dagger & m_f \mathcal{F}_f^\dagger \\ \mathcal{F}_f m_f^\dagger & \mu_F^2 + \mathcal{F}_f \mathcal{F}_f^\dagger \end{pmatrix} \begin{pmatrix} A_f^\dagger & C_f^\dagger \\ B_f^\dagger & D_f^\dagger \end{pmatrix} = \begin{pmatrix} \tilde{m}_f^2 & 0 \\ 0 & \tilde{M}_F^2 \end{pmatrix}, \quad (10)$$

where  $\tilde{m}_f^2$  is a  $3 \times 3$  diagonal matrix in which generation indices are not explicitly written. Equation (10) requires

$$\begin{aligned} m_f m_f^\dagger &= A_f^\dagger \tilde{m}_f^2 A_f + C_f^\dagger \tilde{M}_F^2 C_f, \\ \mathcal{F}_f m_f^\dagger &= B_f^\dagger \tilde{m}_f^2 A_f + D_f^\dagger \tilde{M}_F^2 C_f, \\ \mu_F^2 + \mathcal{F}_f \mathcal{F}_f^\dagger &= B_f^\dagger \tilde{m}_f^2 B_f + D_f^\dagger \tilde{M}_F^2 D_f. \end{aligned} \quad (11)$$

If  $\mu_F^2 + \mathcal{F}_f \mathcal{F}_f^\dagger$  is much larger than each component of  $\mathcal{F}_f m_f^\dagger$ , which can be realized in the case  $u, w \gg \langle \phi \rangle$ , then we find that  $B_f, C_f$ , and  $D_f$  are approximately given as

$$B_f \simeq -\frac{A_f m_f \mathcal{F}_f^\dagger}{\mu_F^2 + \mathcal{F}_f \mathcal{F}_f^\dagger}, \quad C_f \simeq \frac{\mathcal{F}_f m_f^\dagger}{\mu_F^2 + \mathcal{F}_f \mathcal{F}_f^\dagger}, \quad D_f \simeq 1. \quad (12)$$

These guarantee the unitarity of the matrix  $A_f$  within the present experimental bound [3] since  $|B_f|, |C_f| \sim \frac{|m_f|}{|\mathcal{F}_f|} < O(10^{-7})$  is satisfied in each component. In such a case, it is easy to find

$$\begin{aligned} A_f^{-1} \tilde{m}_f^2 A_f &\simeq m_f m_f^\dagger - \frac{1}{\mu_F^2 + \mathcal{F}_f \mathcal{F}_f^\dagger} (m_f \mathcal{F}_f^\dagger) (\mathcal{F}_f m_f^\dagger), \\ \tilde{M}_F^2 &\simeq \mu_F^2 + \mathcal{F}_f \mathcal{F}_f^\dagger. \end{aligned} \quad (13)$$

The right-hand side of the first equation corresponds to an effective squared mass matrix of the ordinary fermions  $f$ . It is derived through the mixing with the extra heavy fermions  $F$ . Since its second term can have complex phases in off-diagonal components as long as  $y_{f_i} \neq \tilde{y}_{f_i}$  is satisfied, the matrix  $A_f$  could be complex. Moreover, if  $\mu_F^2 \lesssim \mathcal{F}_f \mathcal{F}_f^\dagger$  is realized, the complex phase of  $A_f$  in Eq. (13) could have a substantial magnitude because the second term in the right-hand side has a comparable magnitude with the first one. Although it can be realized for various parameter settings, we consider a rather simple situation here<sup>6</sup>:

$$\langle \phi \rangle \ll w < u, \quad y_{f_j} \sim \tilde{y}_{f_j} < y_F. \quad (14)$$

Since the masses of vectorlike fermions are expected to be of  $O(10^8)$  GeV or larger in this case, they decouple from the SM and do not contribute to phenomena at TeV regions.

The CKM matrix is determined as  $V_{\text{CKM}} = O_u^T A_d$ , where  $O_u$  is an orthogonal matrix used for the diagonalization of a mass matrix for up-type quarks. Thus, the  $CP$  phase of  $V_{\text{CKM}}$  is caused by the one of  $A_d$ . The same argument is applied to the leptonic sector, and the PMNS matrix is derived as  $V_{\text{PMNS}} = A_e^\dagger U_\nu$ , where  $U_\nu$  is an orthogonal matrix used for the diagonalization of a neutrino mass matrix. The Dirac  $CP$  phase in the CKM matrix and the PMNS matrix can be induced from the same origin of  $CP$  violation. A concrete example of  $A_d$  is given for a simple case in the Appendix A.

### C. Effective model at a lower energy region

An effective model at lower energy regions than  $w$  and  $u$  can be obtained by integrating out the heavy fields. It is reduced to the SM with a lepton sector extended as the scotogenic neutrino mass model [30], which is characterized by the terms invariant under the remaining  $Z_2$  symmetry

$$\begin{aligned} -\mathcal{L}_{\text{scot}} &= \sum_{\alpha=1}^3 \left[ \sum_{j=1}^3 \left( \tilde{h}_{\alpha j}^* \bar{\ell}_\alpha \eta N_j + \frac{M_{N_j}}{2} \bar{N}_j^c N_j \right) + \sum_{\beta=1}^3 \frac{y_{\alpha\beta}}{M_*} (\bar{\ell}_\alpha \phi) (\bar{\ell}_\beta \phi) + \text{H.c.} \right] \\ &+ \tilde{m}_\phi^2 \phi^\dagger \phi + \tilde{m}_\eta^2 \eta^\dagger \eta + \tilde{\lambda}_1 (\phi^\dagger \phi)^2 + \tilde{\lambda}_2 (\eta^\dagger \eta)^2 + \tilde{\lambda}_3 (\phi^\dagger \phi) (\eta^\dagger \eta) + \lambda_4 (\phi^\dagger \eta) (\eta^\dagger \phi) \\ &+ \frac{\tilde{\lambda}_5}{2} [(\phi^\dagger \eta)^2 + \text{H.c.}], \end{aligned} \quad (15)$$

where neutrino Yukawa couplings  $\tilde{h}_{\alpha j}$  are defined on the basis for which the mass matrix of the charged leptons is diagonalized as discussed in the previous part. Thus, they are complex now. After the spontaneous breaking due to the VEVs of  $\tilde{\sigma}$  and  $\tilde{S}$ , coupling constants in Eq. (15) are related to the ones contained in Eq. (1) as

<sup>6</sup>Leptogenesis could depend on the strength of these couplings heavily in this model as studied later.

$$\begin{aligned}\tilde{\lambda}_1 &= \lambda_1 - \frac{\kappa_{\phi\sigma}^2}{4\tilde{\kappa}_\sigma} - \frac{\kappa_{\phi S}^2}{4\tilde{\kappa}_S} + \frac{\kappa_{\sigma S}\kappa_{\phi\sigma}\kappa_{\phi S}}{4\tilde{\kappa}_\sigma\tilde{\kappa}_S}, & \tilde{\lambda}_2 &= \lambda_2 - \frac{\kappa_{\eta\sigma}^2}{4\tilde{\kappa}_\sigma} - \frac{\kappa_{\eta S}^2}{4\tilde{\kappa}_S} + \frac{\kappa_{\sigma S}\kappa_{\eta\sigma}\kappa_{\eta S}}{4\tilde{\kappa}_\sigma\tilde{\kappa}_S}, \\ \tilde{\lambda}_3 &= \lambda_3 - \frac{\kappa_{\phi\sigma}\kappa_{\eta\sigma}}{2\tilde{\kappa}_\sigma} - \frac{\kappa_{\phi S}\kappa_{\eta S}}{2\tilde{\kappa}_S} + \frac{\kappa_{\sigma S}\kappa_{\phi\sigma}\kappa_{\eta S} + \kappa_{\sigma S}\kappa_{\eta\sigma}\kappa_{\phi S}}{4\tilde{\kappa}_\sigma\tilde{\kappa}_S}, & \tilde{\lambda}_5 &= \lambda_5 \frac{w}{M_*}.\end{aligned}\quad (16)$$

These connection conditions should be imposed at a certain scale  $\bar{M}$ , which is taken to be  $\bar{M} = \tilde{M}_F$  in the present study. Stability of the potential (15) requires the following conditions to be satisfied through scales  $\mu < \bar{M}$ :

$$\tilde{\lambda}_1, \tilde{\lambda}_2 > 0, \quad \tilde{\lambda}_3, \tilde{\lambda}_3 + \lambda_4 - |\tilde{\lambda}_5| > -2\sqrt{\tilde{\lambda}_1\tilde{\lambda}_2}. \quad (17)$$

Potential stability (5) and (17) and perturbativity of the model from the weak scale to the Planck scale can be examined by using renormalization group equations (RGEs) for the coupling constants. Relevant RGEs at  $\mu > \bar{M}$  are given in Appendix B. The mass parameters in Eq. (15) are represented as

$$\begin{aligned}M_{N_j} &= y_{N_j}w, \\ \tilde{m}_\phi^2 &= m_\phi^2 + \left(\kappa_{\phi\sigma} + \frac{\kappa_{\phi S}\kappa_{\sigma S}}{2\tilde{\kappa}_S}\right)w^2 + \left(\kappa_{\phi S} + \frac{\kappa_{\phi\sigma}\kappa_{\sigma S}}{2\tilde{\kappa}_\sigma}\right)u^2, \\ \tilde{m}_\eta^2 &= m_\eta^2 + \left(\kappa_{\eta\sigma} + \frac{\kappa_{\eta S}\kappa_{\sigma S}}{2\tilde{\kappa}_S}\right)w^2 + \left(\kappa_{\eta S} + \frac{\kappa_{\eta\sigma}\kappa_{\sigma S}}{2\tilde{\kappa}_\sigma}\right)u^2.\end{aligned}\quad (18)$$

If  $\tilde{m}_\eta^2 > 0$  is satisfied and  $\eta$  has no VEV, then  $Z_2$  is kept as an exact symmetry of the model. In this model, we assume both  $|\tilde{m}_\phi|$  and  $\tilde{m}_\eta$  have values of  $O(1)$  TeV. Since it has to be realized under the contributions from the VEVs  $w$  and  $u$ , parameter tunings are required.<sup>7</sup>

Phenomenology on neutrinos and DM could be the same as the one that has been studied extensively in various studies [31,32] unless the axion is a dominant component of DM. If the lightest neutral component of  $\eta$  is DM, which is identified as its real component  $\eta_R$ , then both DM relic abundance and DM direct search constrain the parameters  $\tilde{\lambda}_3$  and  $\lambda_4$  [22,33]. As a reference, in Fig. 1 we show their required values in the  $(\lambda_+, \tilde{\lambda}_3)$  plane for the cases  $M_{\eta_R} = 0.9, 1, \text{ and } 1.1$  TeV where  $\lambda_+ = \tilde{\lambda}_3 + \lambda_4 + \tilde{\lambda}_5$  and  $M_{\eta_R}^2 = m_\phi^2 + \lambda_+\langle\phi\rangle^2$ . They should be also consistent with the stability condition (17). The figure shows that these could be satisfied with rather restricted values of  $\tilde{\lambda}_3$  and  $\lambda_4$ . A perturbativity requirement at  $\mu > \bar{M}$  also constrains the model strongly since DM relic abundance requires  $\tilde{\lambda}_3$  and  $|\lambda_4|$  to take rather large values. We have to take account of it to consider the model at high energy regions. As an example, we show the result of RGE study in the right panel of Fig. 1. Details of the assumed initial values are given in Appendix B. If the initial values of  $\tilde{\lambda}_3$  and  $\lambda_4$  are chosen at a larger  $\tilde{\lambda}_3$  region in the left panel, the perturbative condition is violated at a much lower region than the Planck scale. We do not plot the behavior of  $\kappa_i$  in this figure since their values are fixed to be very small and they do not

change their values substantially. If they satisfy the condition (5), it can be confirmed to be kept up to the Planck scale.

Neutrino mass is forbidden at tree level due to this  $Z_2$  symmetry except for the ones generated through dimension five Weinberg operators in Eq. (15). They could give a substantial contribution to the neutrino masses depending on the cutoff scale  $M_*$  and coupling constants  $y_{\alpha\beta}$ . In the present study, however, we assume that their contribution is negligible and the dominant contribution comes from one-loop diagrams with  $\eta$  and  $N_j$  in internal lines. Its formula is given as

$$\mathcal{M}_{\alpha\beta}^\nu \simeq \sum_{j=1}^3 \tilde{h}_{\alpha j} \tilde{h}_{\beta j} \tilde{\lambda}_5 \Lambda_j, \quad \Lambda_j = \frac{\langle\phi\rangle^2}{8\pi^2} \frac{1}{M_{N_j}} \ln \frac{M_{N_j}^2}{M_\eta^2}, \quad (19)$$

where  $M_\eta^2 = \tilde{m}_\eta^2 + (\tilde{\lambda}_3 + \lambda_4)\langle\phi\rangle^2$  and  $M_{N_j} \gg M_\eta$  is supposed. As an example, one may assume a simple flavor structure for neutrino Yukawa couplings [35]

$$\begin{aligned}\tilde{h}_{ei} &= 0, & \tilde{h}_{\mu i} &= \tilde{h}_{\tau i} \equiv h_i \quad (i = 1, 2); \\ \tilde{h}_{e3} &= \tilde{h}_{\mu 3} = -\tilde{h}_{\tau 3} \equiv h_3.\end{aligned}\quad (20)$$

This realizes a tribimaximal mixing, which gives a simple and rather good 0th order approximation for the analysis of neutrino oscillation data and leptogenesis [32]. If we impose the mass eigenvalues obtained from Eq. (19) for the case  $|h_1| \ll |h_2|, |h_3|$  to satisfy the squared mass differences required by the neutrino oscillation data, then we find

<sup>7</sup>For parameter values assumed in this analysis, the order of required tuning is estimated as  $O(10^{-10})$ .

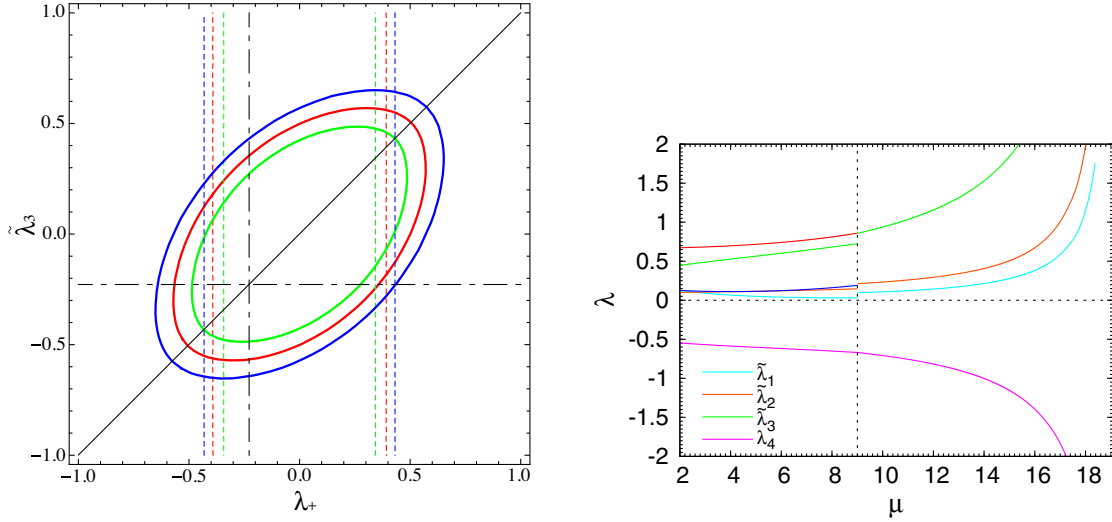


FIG. 1. Left: contours of  $\Omega h^2 = 0.12$  are plotted in the  $(\lambda_+, \tilde{\lambda}_3)$  plane by a solid line for  $M_{\eta_R} = 0.9$  (green), 1 (red), and 1.1 (blue) in a TeV unit. Since  $\eta_R$  should be lighter than the charged components,  $\lambda_4 < 0$  should be satisfied, which corresponds to a region above the diagonal black solid line. Direct search bound from Xenon1T [34] is shown by the same color dashed line for each  $M_{\eta_R}$ . Stability conditions (17) restrict the allowed region to the area marked in the upper right quadrant (marked off by the dot-dashed lines), for which  $\tilde{\lambda}_2 = 0.1$  is assumed. Right: an example of the running of coupling constants  $\tilde{\lambda}_i$  for  $M = 10^\mu$  GeV. Initial values of  $\tilde{\lambda}_3$  and  $\lambda_4$  are fixed as  $\tilde{\lambda}_3 = 0.445$  and  $\lambda_4 = -0.545$ , which are included in the allowed region of the left panel for  $M_{\eta_R} = 1$  TeV.  $\tilde{\lambda}_3 + 2\sqrt{\tilde{\lambda}_1 \tilde{\lambda}_2}$  and  $\lambda_+ + 2\sqrt{\tilde{\lambda}_1 \tilde{\lambda}_2}$  are also plotted by red and blue lines, respectively.

$$|h_2^2 \tilde{\lambda}_5| \Lambda_2 = \frac{1}{2} \sqrt{\Delta m_{32}^2}, \quad |h_3^2 \tilde{\lambda}_5| \Lambda_3 = \frac{1}{3} \sqrt{\Delta m_{21}^2}. \quad (21)$$

Since we have  $\Lambda_{2,3} \sim 7 \times 10^5$  eV for  $M_{2,3} \sim 10^7$  GeV and  $M_\eta \sim 10^3$  GeV, the neutrino oscillation data [3] can be explained by taking as an example

$$y_{N_j} \sim 10^{-2}, \quad |h_2| \sim 6 \times 10^{-3}, \\ |h_3| \sim 2 \times 10^{-3}, \quad |\tilde{\lambda}_5| \sim 10^{-3}. \quad (22)$$

Even if we impose the neutrino oscillation data,  $h_1$  can take a very small value compared with  $h_{2,3}$  [32]. It can play a crucial role for low scale leptogenesis as seen later.

### III. INFLATION DUE TO SINGLET SCALARS

#### A. Inflation

It is well known that a scalar field that couples non-minimally with the Ricci scalar can cause the inflation of the Universe, and the idea has been applied to the Higgs scalar in the SM [17] and its singlet scalar extensions [36,37]. If the singlet scalars  $S$  and  $\sigma$ , which are related to the  $CP$  issues in the SM, couple with the Ricci scalar, then it can play the role of inflaton in this model. The action relevant to the inflation is given in the Jordan frame as

$$S_J = \int d^4x \sqrt{-g} \left[ -\frac{1}{2} M_{\text{pl}}^2 R - \xi_\sigma \sigma^\dagger \sigma R - \xi_{S1} S^\dagger S R - \frac{\xi_{S2}}{2} (S^2 + S^{\dagger 2}) R + \partial^\mu \sigma^\dagger \partial_\mu \sigma + \partial^\mu S^\dagger \partial_\mu S - V(\sigma, S) \right], \quad (23)$$

where  $M_{\text{pl}}$  is the reduced Planck mass and the coupling of  $S$  is controlled by the  $Z_4$  symmetry.  $V(\sigma, S)$  stands for the corresponding part in the potential (1). Since inflation follows very complicated dynamics if multiscalars contribute to it, we confine our study to the inflation in a potential valley. Moreover, we assume  $\xi_{S1} = -\xi_{S2}$  is satisfied for simplicity. In that case, the coupling of  $S$  with the Ricci scalar is reduced to  $\frac{1}{2} \xi_S S_I^2 R$ , where  $S = \frac{1}{\sqrt{2}} (S_R + i S_I)$  and  $\xi_S = \xi_{S1} - \xi_{S2}$ . If  $S$  is supposed to evolve along a constant  $\rho$ , which is determined as a potential minimum  $\frac{\partial V_b}{\partial \rho} = 0$ , then the radial component  $\tilde{S}$  couples with the Ricci scalar as  $\frac{1}{2} \tilde{\xi}_S \tilde{S}^2 R$ , where  $\tilde{\xi}_S$  is defined as  $\tilde{\xi}_S = \xi_S \sin^2 \rho$  and the

potential  $V(\sigma, S)$  is expressed by Eq. (3). Here we consider cases such that both  $\xi_\sigma$  and  $\tilde{\xi}_S$  are positive only. Stability of this potential requires the condition given in Eq. (5). We neglect the VEVs  $w$  and  $u$  for a while since they are much smaller than  $O(M_{\text{pl}})$ , which is the field values of  $\tilde{\sigma}$  and  $\tilde{S}$  during the inflation. We also suppose that other scalars have much smaller values than them.

We consider the conformal transformation for a metric tensor in the Jordan frame

$$\tilde{g}_{\mu\nu} = \Omega^2 g_{\mu\nu}, \quad \Omega^2 = 1 + \frac{(\xi_\sigma \tilde{\sigma}^2 + \tilde{\xi}_S \tilde{S}^2)}{M_{\text{pl}}^2}. \quad (24)$$

After this transformation to the Einstein frame where the Ricci scalar term takes a canonical form, the action can be written as

$$S_E = \int d^4x \sqrt{-\tilde{g}} \left[ -\frac{1}{2} M_{\text{pl}}^2 \tilde{R} + \frac{1}{2} \partial^\mu \chi_\sigma \partial_\mu \chi_\sigma + \frac{1}{2} \partial^\mu \chi_S \partial_\mu \chi_S + \frac{6 \xi_\sigma \tilde{\xi}_S \tilde{\sigma} \tilde{S}}{\left[ \left( \Omega^2 + \frac{6 \xi_\sigma^2}{M_{\text{pl}}^2} \tilde{\sigma}^2 \right) \left( \Omega^2 + \frac{6 \tilde{\xi}_S^2}{M_{\text{pl}}^2} \tilde{S}^2 \right) \right]^{1/2}} \partial^\mu \chi_\sigma \partial_\mu \chi_S - \frac{1}{\Omega^4} V(\tilde{\sigma}, \tilde{S}) \right], \quad (25)$$

where  $\chi_\sigma$  and  $\chi_S$  are defined as [36]

$$\begin{aligned} \frac{\partial \chi_\sigma}{\partial \tilde{\sigma}} &= \frac{1}{\Omega^2} \sqrt{\Omega^2 + 6 \xi_\sigma^2 \frac{\tilde{\sigma}^2}{M_{\text{pl}}^2}}, \\ \frac{\partial \chi_S}{\partial \tilde{S}} &= \frac{1}{\Omega^2} \sqrt{\Omega^2 + 6 \tilde{\xi}_S^2 \frac{\tilde{S}^2}{M_{\text{pl}}^2}}. \end{aligned} \quad (26)$$

If we introduce variables  $\tilde{\chi}$ ,  $\varphi$  to express  $\tilde{\sigma}$  and  $\tilde{S}$  as  $\tilde{\sigma} = \tilde{\chi} \cos \varphi$ ,  $\tilde{S} = \tilde{\chi} \sin \varphi$ , then the potential in the Einstein frame at the large field regions such as  $\xi_\sigma \tilde{\sigma}^2 + \tilde{\xi}_S \tilde{S}^2 \gg M_{\text{pl}}^2$  can be written as

$$V(\tilde{\chi}, \varphi) = \frac{M_{\text{pl}}^4 \tilde{\kappa}_S \sin^4 \varphi + \tilde{\kappa}_\sigma \cos^4 \varphi + \kappa_{\sigma S} \sin^2 \varphi \cos^2 \varphi}{4 (\xi_\sigma \cos^2 \varphi + \tilde{\xi}_S \sin^2 \varphi)^2}. \quad (27)$$

We find that there are three types of valley along the minimum in the  $\varphi$  direction of this potential. They realize different types of inflaton. Two of them are

$$\begin{aligned} \text{(i)} \quad \varphi &= 0 \quad \text{for } 2\tilde{\kappa}_\sigma \tilde{\xi}_S < \kappa_{\sigma S} \xi_\sigma, \\ \text{(ii)} \quad \varphi &= \frac{\pi}{2} \quad \text{for } 2\tilde{\kappa}_S \xi_\sigma < \kappa_{\sigma S} \tilde{\xi}_S. \end{aligned} \quad (28)$$

In each case, a kinetic term mixing between  $\chi_\sigma$  and  $\chi_S$  disappears and inflaton can be identified with  $\chi_\sigma$  for (i) and  $\chi_S$  for (ii), respectively.<sup>8</sup>

Another valley that is studied in this paper is realized at

$$\sin^2 \varphi = \frac{2\tilde{\kappa}_\sigma \tilde{\xi}_S - \kappa_{\sigma S} \xi_\sigma}{(2\tilde{\kappa}_S \xi_\sigma - \kappa_{\sigma S} \tilde{\xi}_S) + (2\tilde{\kappa}_\sigma \tilde{\xi}_S - \kappa_{\sigma S} \xi_\sigma)}, \quad (29)$$

under the conditions

$$2\tilde{\kappa}_\sigma \tilde{\xi}_S > \kappa_{\sigma S} \xi_\sigma, \quad 2\tilde{\kappa}_S \xi_\sigma > \kappa_{\sigma S} \tilde{\xi}_S, \quad (30)$$

where we note that these are automatically satisfied for  $\kappa_{\sigma S} < 0$  since Eq. (5) is imposed, and  $\tilde{\xi}_S$  and  $\xi_\sigma$  are assumed to be positive. In this case the inflaton  $\tilde{\chi}$  is a mixture of  $\tilde{\sigma}$  and  $\tilde{S}$  with a constant value of  $\tilde{\sigma}/\tilde{S}$ . Although the kinetic term mixing cannot be neglected for a general  $\sin \varphi$ , it can be safely neglected if we restrict it to the one in which the

<sup>8</sup>In different context, the inflaton dominated by  $\tilde{\sigma}$  and the  $\tilde{S}$  inflaton have been discussed in [38,11], respectively.

inflaton is dominated by  $\tilde{S}$  ( $\sin^2 \varphi \simeq 1$ ) or  $\tilde{\sigma}$  ( $\sin^2 \varphi \simeq 0$ ). We focus our study on the former case where  $\tilde{\chi} \gg \tilde{\sigma}$  is always satisfied during inflation. If we additionally impose  $\tilde{\xi}_S \gg \xi_\sigma$  on Eq. (29) and assume that the relevant couplings satisfy

$$\kappa_{\sigma S} < 0, \quad \tilde{\kappa}_S < |\kappa_{\sigma S}| < \tilde{\kappa}_\sigma, \quad (31)$$

$\sin \varphi$  is expressed as  $\sin^2 \varphi = 1 + \frac{\kappa_{\sigma S}}{2\tilde{\kappa}_\sigma}$ . In this case, by using  $\hat{\kappa}_S = \tilde{\kappa}_S - \frac{\kappa_{\sigma S}^2}{4\tilde{\kappa}_\sigma}$ , potential can be expressed as  $V(\tilde{S}) = \frac{1}{4\Omega^4} \hat{\kappa}_S \tilde{S}^4$  at the bottom of the valley and  $\cos 2\rho = -\frac{\beta}{4\alpha} \cot^2 \varphi$  realizes the minimum of  $V_b$  if  $\tan^2 \varphi > |\frac{\beta}{4\alpha}|$  is satisfied. Nature of the inflaton  $\tilde{\chi}$  is fixed by the parameters  $\tilde{\kappa}_S$ ,  $\tilde{\kappa}_\sigma$ , and  $\kappa_{\sigma S}$ .

Squared mass of the orthogonal component to  $\tilde{\chi}$  during inflation can be estimated as  $m_{\tilde{\chi}_\perp}^2 = \frac{|\kappa_{\sigma S}| M_{\text{pl}}^2}{2\tilde{\xi}_S^2}$ . Since the Hubble parameter  $H_I$  satisfies  $H_I^2 = \frac{\hat{\kappa}_S M_{\text{pl}}^2}{12\tilde{\xi}_S^2}$  at the same period,  $H_I < m_{\tilde{\chi}_\perp}$  is satisfied under the condition (31).<sup>10</sup> Thus, the inflation  $\chi$  starts rolling along the valley within a few Hubble time independently of an initial value of the inflaton. It justifies our analyzing the model as a single field inflation model. On the other hand, since  $\tilde{\sigma} (= \sqrt{\frac{|\kappa_{\sigma S}|}{2\tilde{\kappa}_\sigma}} \tilde{\chi}) > \frac{H_I}{\sqrt{2\pi}}$  is satisfied generally,<sup>11</sup> the global  $U(1)$  is spontaneously broken during inflation, and isocurvature fluctuation could be problematic [38]. However, even in that case it is escapable since the axion needs not to be a dominant component of DM in the present model. This problem is discussed later.

The canonically normalized inflaton  $\chi$  can be expressed as [38]

<sup>9</sup>If we assume  $\tilde{\kappa}_S > |\kappa_{\sigma S}|$ , then  $\sin \varphi$  is differently expressed as  $\sin^2 \varphi = 1 - \frac{\tilde{\kappa}_S \xi_\sigma}{\tilde{\kappa}_\sigma \tilde{\xi}_S}$ . However, we do not consider such a case in this paper.

<sup>10</sup>Mass of another orthogonal component  $S_I$  is estimated as  $m_{S_I}^2 \sim \frac{8\alpha M_{\text{pl}}^2}{\tilde{\xi}_S^2}$  for a case  $\cos 2\rho \sim 0$ , which is interested in the present study and then  $96\alpha > \hat{\kappa}_S$  is required for  $m_{S_I} > H_I$ . Although  $\alpha \ll \hat{\kappa}_S$  is assumed from the vacuum determination, it can be satisfied for suitable values of  $\alpha$ .

<sup>11</sup>Although it may be escapable for  $\tilde{\xi}_S \ll \sqrt{|\kappa_{\sigma S}|}$ , it is not the case in the present model.



$$\Omega^2 \frac{d\chi}{d\tilde{S}} = \sqrt{\gamma\Omega^2 + 6\tilde{\xi}_S^2 \frac{\tilde{S}^2}{M_{\text{pl}}^2}}, \quad (32)$$

where  $\gamma$  can be approximated along the valley as

$$\gamma = 1 - \frac{\kappa_{\sigma S}}{2\tilde{\kappa}_\sigma}. \quad (33)$$

If we use  $\gamma \simeq 1$ , then the potential of  $\chi$  obtained through  $V(\chi) = \frac{1}{\Omega^4} V(\tilde{\sigma}, \tilde{S})$  can be derived by using the solution of Eq. (32), which is given as

$$\begin{aligned} \frac{\chi}{M_{\text{pl}}} = & -\sqrt{6} \operatorname{arcsinh} \left( \frac{\sqrt{\frac{6}{\gamma} \frac{\tilde{\xi}_S \tilde{S}}{M_{\text{pl}}}}}{\sqrt{1 + \frac{\tilde{\xi}_S}{M_{\text{pl}}^2} \tilde{S}^2}} \right) \\ & + \sqrt{\frac{\gamma + 6\tilde{\xi}_S}{\tilde{\xi}_S}} \operatorname{arcsinh} \left( \frac{\sqrt{\frac{\tilde{\xi}_S}{\gamma} (1 + \frac{6}{\gamma} \frac{\tilde{\xi}_S}{M_{\text{pl}}^2} \tilde{S}^2)}}{M_{\text{pl}}} \right). \end{aligned} \quad (34)$$

We derive the potential of  $\chi$  through numerical calculation for a typical value of  $\tilde{\xi}_S$  by using Eq. (34). Such examples of  $V(\chi)$  are shown in Fig. 2. It can be approximated as

$$V(\chi) = \begin{cases} \frac{\hat{\kappa}_S}{4\tilde{\xi}_S^2} M_{\text{pl}}^4 & \chi > M_{\text{pl}} \\ \frac{\hat{\kappa}_S}{6\tilde{\xi}_S^2} M_{\text{pl}}^2 \chi^2 & \frac{M_{\text{pl}}}{\tilde{\xi}_S} < \chi < M_{\text{pl}} \\ \frac{\hat{\kappa}_S}{4} \chi^4 & \chi < \frac{M_{\text{pl}}}{\tilde{\xi}_S} \end{cases} \quad (35)$$

The inflation ends at  $\chi_{\text{end}} \simeq M_{\text{pl}}$ . After the end of inflation, there is a substantial region where the potential behaves as a quadratic form before it is reduced to a quartic form at low energy regions for the case  $\tilde{\xi}_S \gg 1$  as in the Higgs inflation. However, such a region can be neglected for the case  $\tilde{\xi}_S < 10$ , which is the case considered in this study. Since the inflaton oscillating in the quartic potential behaves as radiation as shown later, the radiation domination starts soon after the end of inflation in that case.

The slow-roll parameters in this model can be estimated by using Eq. (32) as [16]

$$\begin{aligned} \epsilon & \equiv \frac{M_{\text{pl}}^2}{2} \left( \frac{V'}{V} \right)^2 = \frac{8M_{\text{pl}}^4}{\gamma\tilde{\xi}_S(1 + \frac{6}{\gamma} \frac{\tilde{\xi}_S}{M_{\text{pl}}^2} \tilde{S}^2)^4}, \\ \eta & \equiv M_{\text{pl}}^2 \frac{V''}{V} = -\frac{8M_{\text{pl}}^2}{\gamma(1 + \frac{6}{\gamma} \frac{\tilde{\xi}_S}{M_{\text{pl}}^2} \tilde{S}^2)}. \end{aligned} \quad (36)$$

The  $e$ -foldings number  $\mathcal{N}_k$  from the time when the scale  $k$  exits the horizon to the end of inflation is estimated by using Eq. (32) as

$$\begin{aligned} \mathcal{N}_k & = \frac{1}{M_{\text{pl}}^2} \int_{\chi_{\text{end}}}^{\chi_k} \frac{V}{V'} d\chi \\ & = \frac{1}{8M_{\text{pl}}^2} (\gamma + 6\tilde{\xi}_S) (\tilde{S}_k^2 - \tilde{S}_{\text{end}}^2) - \frac{3}{4} \ln \frac{M_{\text{pl}}^2 + \tilde{\xi}_S \tilde{S}_k^2}{M_{\text{pl}}^2 + \tilde{\xi}_S \tilde{S}_{\text{end}}^2}. \end{aligned} \quad (37)$$

Taking account of these, the slow-roll parameters in this inflation scenario is found to be approximated as  $\epsilon \simeq \frac{3}{4\mathcal{N}_k^2}$  and  $\eta \simeq -\frac{1}{\mathcal{N}_k}$ . The field value of inflaton during the inflation is found to be expressed as  $\chi_k = \frac{\sqrt{6}}{2} M_{\text{pl}} \ln(32\tilde{\xi}_S \mathcal{N}_k)$  by using Eqs. (34) and (37), and its potential  $V_k(\equiv V(\chi_k))$  takes a constant value as shown in Eq. (35). On the other hand, if we use  $\epsilon = 1$  at the end of inflation, then the inflaton potential is estimated as  $V_{\text{end}}(\equiv V(\chi_{\text{end}})) \simeq 0.072 \frac{\hat{\kappa}_S}{\tilde{\xi}_S^2} M_{\text{pl}}^4$ , which is found to be a good approximation from Fig. 2.

The spectrum of density perturbation predicted by the inflation is known to be expressed as [16]

$$\mathcal{P}(k) = A_s \left( \frac{k}{k_*} \right)^{n_s-1}, \quad A_s = \frac{V}{24\pi^2 M_{\text{pl}}^4 \epsilon} \Big|_{k_*}. \quad (38)$$

If we use the Planck data  $A_s = (2.101_{-0.034}^{+0.031}) \times 10^{-9}$  at  $k_* = 0.05 \text{ Mpc}^{-1}$  [15], then we find the Hubble parameter during the inflation to be  $H_I = 1.4 \times 10^{13} (\frac{60}{\mathcal{N}_{k_*}}) \text{ GeV}$  and the relation

$$\hat{\kappa}_S \simeq 4.13 \times 10^{-10} \tilde{\xi}_S^2 \left( \frac{60}{\mathcal{N}_{k_*}} \right)^2, \quad (39)$$

which should be satisfied at the horizon exit time of the scale  $k_*$ . We confine our study to the case  $\tilde{\xi}_S < 10$ .

In Fig. 3, we plot predicted values for the scalar spectral index  $n_s$  and the tensor-to-scalar ratio  $r$  in the present model. Since the quartic coupling  $\hat{\kappa}_S$  is a free parameter of the model under the constraint (39), we vary  $\hat{\kappa}_S$  in the range  $10^{-10} \leq \hat{\kappa}_S \leq 10^{-7}$  for fixed values of  $\tilde{\xi}_S$  or  $\mathcal{N}_k$ . The CMB constraint (39) is satisfied at intersection points of the lines with a fixed value of  $\tilde{\xi}_S$  or  $\mathcal{N}_k$ . The figure shows that the constraints of the observed CMB data [15] are satisfied for the supposed parameters.

After the end of inflation, the inflaton  $\chi$  starts oscillation in the potential  $V(\chi)$ . At this stage, the description by  $\chi$  is no longer justified, especially, at the small field regions.  $\varphi$  is not constant in general there.  $\tilde{S}$  and  $\tilde{\sigma}$  should be treated independently. In the following study, however, we confine our study to a special inflaton trajectory and estimate the reheating phenomena by using  $\chi$  to give a rough evaluation of reheating temperature under the assumption that inflaton follows a constant  $\varphi$  trajectory.<sup>12</sup> In this case, inflaton oscillation is described by the equation

$$\frac{d^2\chi}{dt^2} + 3H \frac{d\chi}{dt} + V'(\chi) = 0. \quad (40)$$

<sup>12</sup>During the first several oscillations, both  $\varphi$  and  $\rho$  can be numerically confirmed to take constant values. This suggests that single field treatment is rather good during the first few oscillations at least.

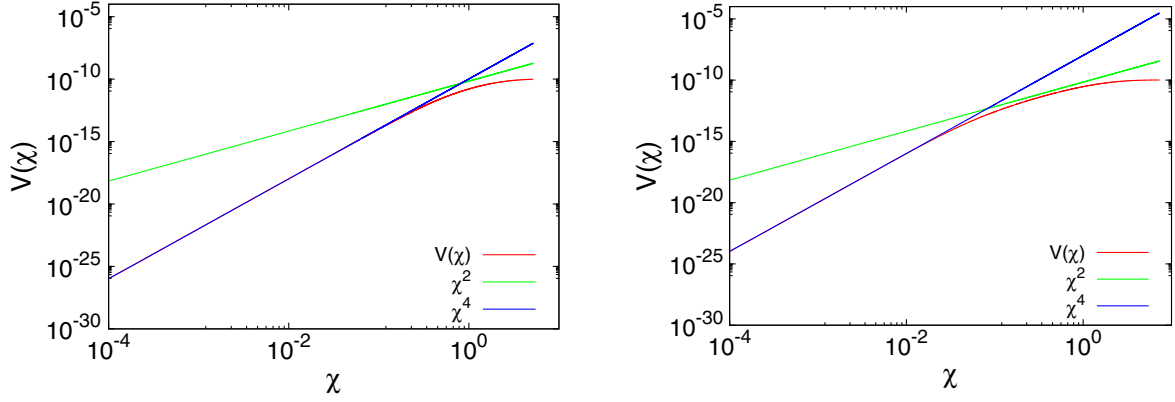


FIG. 2. Potential of the inflaton  $\chi$  for  $\tilde{\xi}_S = 1$  (left panel) and  $\tilde{\xi}_S = 10$  (right panel). In both panels,  $\tilde{\xi}_S/\xi_\sigma = 20$  and  $\tilde{\kappa}_S/|\kappa_{\sigma S}| = |\kappa_{\sigma S}|/\tilde{\kappa}_\sigma = 0.1$  are assumed and  $\tilde{\kappa}_S$  is fixed by using Eq. (39) for  $\mathcal{N}_k = 55$ . As references, we also plot approximated potential  $\frac{\tilde{\kappa}_S}{6\tilde{\xi}_S} M_{\text{pl}}^2 \chi^2$  and  $\frac{\tilde{\kappa}_S}{4} \chi^4$  in Eq. (35) as  $\chi^2$  and  $\chi^4$ . In these plots, a Planck unit ( $M_{\text{pl}} = 1$ ) is used.

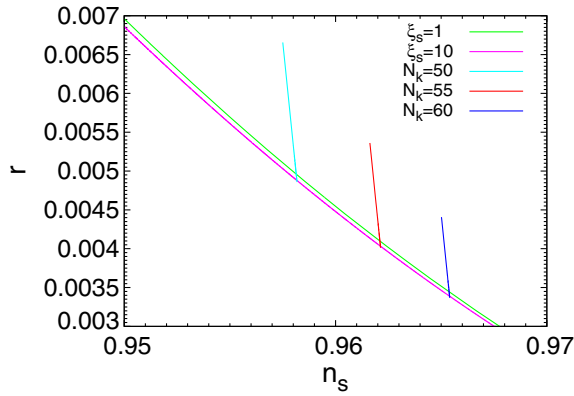


FIG. 3. Predicted values of the scalar spectral index  $n_s$  and the tensor-to-scalar ratio  $r$  in this model. They are read off as the values at intersection points of two lines with a fixed value of  $\tilde{\xi}_S$  or  $\mathcal{N}_k$ . The coupling constant  $\tilde{\kappa}_S$  is varied in a range from  $10^{-7}$  to  $10^{-10}$ .

Since the amplitude of  $\chi$  evolves approximately as  $\Phi(t) = \frac{\tilde{\xi}_S}{\sqrt{\pi\tilde{\kappa}_S t}}$  in the quadratic potential after the end of inflation, the inflaton  $\chi$  oscillates  $\frac{1}{2\pi\sqrt{3\pi}}(\tilde{\xi}_S - 1)$  times before the potential (35) changes from a quadratic form to a quartic one. This means that preheating under the quadratic potential could play no substantial role for the case  $\tilde{\xi}_S < 10$ . In such a case, we need to consider the preheating in the quartic potential only. The model with the quartic potential  $V(\chi) = \frac{\tilde{\kappa}_S}{4}\chi^4$  becomes conformally invariant [39].

If we introduce dimensionless conformal time  $\tau$ , which is defined by using a scale factor  $a$  as  $a d\tau = \sqrt{\tilde{\kappa}_S} \chi_{\text{end}} dt$  and also a rescaled field  $f = \frac{a\chi}{\chi_{\text{end}}}$ , then Eq. (40) can be rewritten as

$$\frac{d^2 f}{d\tau^2} + f^3 = 0. \quad (41)$$

The solution of this equation which describes the inflaton oscillation is known to be given by a Jacobi elliptic function  $f(\tau) = \text{cn}(\tau - \tau_i, \frac{1}{\sqrt{2}})$ .<sup>13</sup> From the Friedman equation for this inflaton oscillation, we find

$$a(\tau) = \frac{\chi_{\text{end}}}{2\sqrt{3}M_{\text{pl}}} \tau, \quad \tau = 2(3\tilde{\kappa}_S M_{\text{pl}}^2)^{1/4} \sqrt{t}. \quad (42)$$

Since  $H = 1/2t$  is satisfied, this oscillation era is radiation dominated. If we take into account such a feature of the model that radiation domination starts just after the end of inflation, the  $e$ -foldings number  $\mathcal{N}_k$  can be expressed by noting a relation  $k = a_k H_k$  as

$$\mathcal{N}_k = 56.7 - \ln\left(\frac{k}{a_0 H_0}\right) + \ln\left(\frac{V_{\text{end}}^{1/4}}{10^{14} \text{ GeV}}\right) + 2 \ln\left(\frac{V_k^{1/4}}{V_{\text{end}}^{1/4}}\right), \quad (43)$$

where  $H_k^2 = \frac{V_k}{3M_{\text{pl}}^2}$  and the suffix 0 stands for the present value of each quantity. Reheating temperature dependence of  $\mathcal{N}_k$  is weak or lost differently from the usual case [16] where substantial matter domination is assumed to follow the inflation era.<sup>14</sup> In the next part, we discuss the reheating temperature expected to be realized in the present model.

<sup>13</sup>If we take  $\tau_i \simeq 2.44$ , then  $f(\tau)$  can be approximated by  $\cos(\frac{2\pi}{\tau_0} \tau)$ , where  $\tau_0$  is expressed by using the complete elliptic integral of the first kind  $K$  as  $\tau_0 = 4K(\frac{1}{\sqrt{2}})$  [39].

<sup>14</sup>If reheating occurs through a perturbative process at  $\chi \lesssim u$  where matter domination is realized, its effect on  $\mathcal{N}_k$  could also be negligible as long as  $\Gamma > H$  is satisfied at that stage where  $\Gamma$  is inflaton decay width.

## B. Preheating and reheating

Before proceeding to the study of particle production under the background oscillation of inflaton, we need to know the mass of the relevant particles, which is induced through the interaction with inflaton. Such interactions are given as

$$\begin{aligned} & \left[ -\frac{y_D}{\sqrt{2}} \frac{\kappa_{\sigma S}}{2\tilde{\kappa}_\sigma} \chi \bar{D}_L D_R - \frac{y_E}{\sqrt{2}} \frac{\kappa_{\sigma S}}{2\tilde{\kappa}_\sigma} \chi \bar{E}_L E_R + \sum_{j=1}^3 \left\{ \frac{1}{\sqrt{2}} (y_{d_j} e^{i\rho} + \tilde{y}_{d_j} e^{-i\rho}) \chi \bar{D}_L d_{R_j} \right. \right. \\ & \left. \left. + \frac{1}{\sqrt{2}} (y_{e_j} e^{i\rho} + \tilde{y}_{e_j} e^{-i\rho}) \chi \bar{E}_L e_{R_j} - \frac{y_{N_j}}{2\sqrt{2}} \frac{\kappa_{\sigma S}}{2\tilde{\kappa}_\sigma} \chi \bar{N}_j^c N_j \right\} + \text{H.c.} \right] \\ & + \frac{1}{2} (\kappa_{\phi S} \phi^\dagger \phi + \kappa_{\eta S} \eta^\dagger \eta) \chi^2 - \frac{\kappa_{\sigma S}}{2\tilde{\kappa}_\sigma} (\kappa_{\phi\sigma} \phi^\dagger \phi + \kappa_{\phi\sigma} \eta^\dagger \eta) \chi^2. \end{aligned} \quad (44)$$

The particles interacting with the inflaton  $\chi$  have mass varying with the oscillation of  $\chi$  and their mass can be read off from Eq. (44) as

$$\begin{aligned} M_{N_j} & \simeq \frac{y_{N_j} |\kappa_{\sigma S}|}{\sqrt{2}} \frac{\chi}{2\tilde{\kappa}_\sigma}, & \tilde{M}_F & \simeq \frac{\chi}{\sqrt{2}} \left[ \sum_{j=1}^3 (y_{f_j}^2 + \tilde{y}_{f_j}^2) + y_F^2 \frac{\kappa_{\sigma S}^2}{4\tilde{\kappa}_\sigma^2} \right]^{\frac{1}{2}}, \\ m_\phi^2 & \simeq \frac{1}{2} \left( \kappa_{\phi S} + \frac{|\kappa_{\sigma S}|}{\tilde{\kappa}_\sigma} \kappa_{\phi\sigma} \right) \chi^2, & m_\eta^2 & \simeq \frac{1}{2} \left( \kappa_{\eta S} + \frac{|\kappa_{\sigma S}|}{\tilde{\kappa}_\sigma} \kappa_{\eta\sigma} \right) \chi^2, \end{aligned} \quad (45)$$

where  $F = D$  or  $E$  should be understood for  $f = d$  or  $e$ , respectively. Since the effect of nonminimal coupling is negligible during this oscillation period, it is convenient to use the components of  $\sigma$  and  $S$ , which are parallel and orthogonal to the inflaton  $\chi$  to describe their interactions. If we indicate each of them as  $\sigma_\parallel$ ,  $\sigma_\perp$ ,  $S_\parallel$ , and  $S_\perp$ , then their interactions are expressed as

$$\begin{aligned} & \frac{\tilde{\kappa}_S}{4} (S_\parallel^2 + S_\perp^2 - u^2)^2 + \frac{\kappa_{\sigma S}}{4} (S_\parallel^2 + S_\perp^2 - u^2) (\sigma_\parallel^2 + \sigma_\perp^2 - w^2) \\ & + \frac{\tilde{\kappa}_\sigma}{4} (\sigma_\parallel^2 + \sigma_\perp^2 - w^2)^2. \end{aligned} \quad (46)$$

By combining these interactions with the composition of  $\chi$ , their masses are found to be given by<sup>15</sup>

$$\begin{aligned} m_{S_\parallel}^2 & \simeq \left( 3\hat{\kappa}_S + \frac{\kappa_{\sigma S}^2}{2\tilde{\kappa}_\sigma} \right) \chi^2, & m_{\sigma_\parallel}^2 & \simeq \left( |\kappa_{\sigma S}| + \frac{\kappa_{\sigma S}^2}{4\tilde{\kappa}_\sigma} \right) \chi^2, \\ m_{S_\perp}^2 & \simeq \hat{\kappa}_S \chi^2, & m_{\sigma_\perp}^2 & \simeq \frac{\kappa_{\sigma S}^2}{4\tilde{\kappa}_\sigma} \chi^2. \end{aligned} \quad (47)$$

The coupling constants relevant to these masses are restricted through the assumed inflaton composition and the realization of the  $CP$  phases in the CKM and PMNS matrices. The discussion in the previous sections shows that such requirements are satisfied for

<sup>15</sup>It should be noted that the mass of  $\sigma$  could have another non-negligible contribution that is induced by explicit breaking of the global  $U(1)$  symmetry brought about by the quantum gravitational effects. We do not take account of it in the present study.

$$\hat{\kappa}_S < |\kappa_{\sigma S}| < \tilde{\kappa}_\sigma, \quad \hat{\kappa}_S < y_{N_j}, y_{f_j}, \tilde{y}_{f_j}. \quad (48)$$

We assume additionally

$$\hat{\kappa}_S < g_\phi \equiv \kappa_{\phi S} + \frac{|\kappa_{\sigma S}|}{\tilde{\kappa}_\sigma} \kappa_{\phi\sigma}, \quad \hat{\kappa}_S < g_\eta \equiv \kappa_{\eta S} + \frac{|\kappa_{\sigma S}|}{\tilde{\kappa}_\sigma} \kappa_{\eta\sigma}. \quad (49)$$

Since the oscillation frequency of the inflaton is  $\sim \sqrt{\tilde{\kappa}_S} \chi$ , decays or annihilations of the inflaton are kinematically forbidden except for the one to  $\sigma_\perp$  as found from Eqs. (45) and (47). In  $\sigma_\perp$  case, the inflaton reaction rate to it is much smaller than the Hubble parameter at this period because of the smallness of its coupling with the inflaton, energy drain from the inflaton to  $\sigma_\perp$  is ineffective to be neglected. As a result, the energy transfer from the inflaton oscillation to excited particles is expected to occur at the time when the inflaton crosses the zero where the resonant particle production is possible.

Preheating under the background inflaton oscillation can generate the excitations of  $\chi$  itself and other scalars  $\psi$  which couple with  $\chi$  at its zero crossing [40]. In a quartic potential case [39], the model becomes conformally invariant and the time evolution equations of  $\chi_k (\simeq S_k)$  and  $\psi_k$ , which are the comoving modes with a momentum  $k$ , can be transformed to the simple ones by rescaling them to the dimensionless quantities in the same way as Eq. (41). They are given as

$$\begin{aligned} \frac{d^2}{d\tau^2} X_k + \omega_k^2 X_k & = 0, & \omega_k^2 & = \bar{k}^2 + 3f(\tau)^2, \\ \frac{d}{d\tau^2} F_k + \tilde{\omega}_k^2 F_k & = 0, & \tilde{\omega}_k^2 & = \bar{k}^2 + \frac{g_\psi}{\hat{\kappa}_S} f(\tau)^2, \end{aligned} \quad (50)$$

where the rescaled variables are defined as

$$X_k = \frac{a\chi_k}{\chi_{\text{end}}}, \quad F_k = \frac{a\psi_k}{\chi_{\text{end}}}, \quad \bar{k} = \frac{ak}{\chi_{\text{end}}\sqrt{\hat{\kappa}_S}}. \quad (51)$$

Function  $f(\tau)$  is the solution of Eq. (41) and  $g_\psi$  stands for a coupling constant of the relevant particle  $\psi (= \sigma, S_\perp, \phi, \eta)$  with the inflaton  $\chi$ , which can read off from Eqs. (45) and (47). Amplitudes  $X_k$  and  $F_k$  are known to show the exponential behavior  $\propto e^{\mu_k \tau}$  with a characteristic exponent  $\mu_k$ , which is determined by a parameter  $g_\psi/\hat{\kappa}_S$ . Using the solutions of Eq. (50), the number density of the produced particle  $\psi$  can be calculated as

$$n_k^\psi = \frac{\tilde{\omega}_k}{2\hat{\kappa}_S} \left( \frac{|F'_k|^2}{\tilde{\omega}_k^2} + |F_k|^2 \right) - \frac{1}{2}. \quad (52)$$

Particle production based on Eq. (50) at the inflaton zero crossing has been studied in [39] and it is shown to be characterized by the parameter  $g_\psi/\hat{\kappa}_S$ . We classify the relevant couplings into five groups

$$\begin{aligned} \text{(A)} \quad \frac{g_{\sigma_\parallel}}{\hat{\kappa}_S} \gg 1, & \quad \text{(B)} \quad \frac{g_{S_\parallel}}{\hat{\kappa}_S} = 3, & \quad \text{(C)} \quad \frac{g_{S_\perp}}{\hat{\kappa}_S} = 1, \\ \text{(D)} \quad \frac{g_{\sigma_\perp}}{\hat{\kappa}_S} \ll 1, & \quad \text{(E)} \quad \frac{g_\phi}{\hat{\kappa}_S}, \frac{g_\eta}{\hat{\kappa}_S} > 1, \end{aligned} \quad (53)$$

where we note that couplings in (A)–(D) are fixed by the present inflaton composition but the ones in (E) are not constrained. Now we consider the resonant particle production in each group. A maximum value of characteristic exponent in (D) is very small so that it plays no effective role also in preheating. In (B) and (C), both the fluctuations of  $S_\parallel$  and  $S_\perp$  are produced fast, but it stops as soon as  $\langle |S_\parallel|^2 \rangle$  and  $\langle |S_\perp|^2 \rangle$  reach a certain value such as  $0.5\chi_{\text{end}}^2/a^2$ . Although a maximum value  $\mu_{\text{max}}$  of the characteristic exponent of (B) is much smaller than the one of (C) and also the resonance band of (B) is much narrower than (C), the interaction  $S_\parallel^2 S_\perp^2$  accelerates the production of fluctuations of  $S_\parallel$  through rescattering and they reach the similar value [38,41]. Since the backreaction of these fluctuations to the inflaton oscillation restructures the resonance band, the resonant particle production stops before causing much more conversion of the inflaton oscillation energy to particle excitations. Moreover, since the decay of excitations produced through these processes are also closed kinematically, these could not play an efficient role in reheating. In (A), since  $\sigma_\parallel$  also couples to the inflaton directly, the resonant production of its excitation stops at a certain stage due to the same reason as (B) and (C). Even if the excited particles are allowed to decay to fermions  $F$  and  $N_j$  kinematically, the decay width is much smaller than the Hubble parameters to be neglected. As a result, if the process due to (E) is not effective, preheating cannot play

any role for reheating and reheating proceeds through perturbative processes after the amplitude of inflaton is smaller than the VEV  $u$ .

Here, we have to note that there is a possibility in (E) where the energy transfer from the inflaton oscillation to radiation proceeds through preheating since the produced excitations can decay to relativistic particles differently from (B) and (C). In this case,  $\phi$  and  $\eta$  are produced as excitations at the zero crossing of the inflaton where an adiabaticity condition  $\tilde{\omega}'_k < \tilde{\omega}_k^2$  could be violated for certain values of  $\bar{k}$ . By using the analytic solution of Eq. (50) derived in [39], the momentum distribution  $n_k^\psi$  of the produced particle  $\psi$  through one zero crossing of the inflaton can be estimated as

$$n_k^\psi = e^{2\mu_k \frac{\tau_0}{2}} = e^{-(\bar{k}/\bar{k}_c)^2}, \quad \bar{k}_c^2 = \sqrt{\frac{g_\psi}{2\pi^2 \hat{\kappa}_S}}, \quad (54)$$

where  $\tau_0$  is an inflaton oscillation period and  $\tau_0 = 7.416$ . The resonance is efficient for  $\bar{k} < \bar{k}_c$ . Thus, the particle number density produced during one zero crossing of the inflaton is

$$\bar{n}^\psi = \int \frac{d^3\bar{k}}{(2\pi)^3} n_k^\psi = \int \frac{d^3\bar{k}}{(2\pi)^3} e^{-(\bar{k}/\bar{k}_c)^2} = \frac{\bar{k}_c^3}{8\pi^{3/2}}. \quad (55)$$

The energy transfer from the inflaton oscillation to relativistic particles is caused through the decay of the produced particles  $\psi (= \phi, \eta)$  and thermalization proceeds. They can decay to light fermions through  $\phi \rightarrow \bar{q}t$  with a top Yukawa coupling  $h_t$  and  $\eta \rightarrow \bar{\ell}N$  with neutrino Yukawa couplings  $h_j$ , respectively. Here, we should note that  $\eta$  can be heavier than  $N_j$  at this stage even if  $\eta$  is the lightest one with  $Z_2$  odd parity at the weak scale. It is caused by the inflaton composition in the present model as found from Eq. (45). Their decay widths in the comoving frame are given by using the conformally rescaled unit as

$$\bar{\Gamma}_\psi = \frac{c_\psi y_\psi^2}{8\pi} \bar{m}_\psi, \quad \bar{m}_\psi = \frac{am_\psi}{\chi_{\text{end}}\sqrt{\hat{\kappa}_S}} = \sqrt{\frac{g_\psi}{\hat{\kappa}_S}} f(\tau), \quad (56)$$

where  $\psi = \phi, \eta$ , and  $c_\psi$  are internal degrees of freedom  $c_\phi = 3$  and  $c_\eta = 1$ . The Yukawa coupling  $y_\psi$  represents  $y_\phi = h_t$  and  $y_\eta = h_j$ . Since  $\bar{\Gamma}_\psi^{-1} < \tau_0/2$  is satisfied for  $g_\psi > 4 \times 10^{-7} (\frac{\hat{\kappa}_S}{10^{-8}})$ , the produced  $\psi$  decays to the light fermions completely before the next inflaton zero crossing [42], and then it is not accumulated in such cases. We fix  $\tau = 0$  at the first inflaton zero crossing so that  $f(\tau)$  can be expressed approximately as  $f(\tau) = f_0 \sin(cf_0\tau)$ . Transferred energy density through the  $\psi$  decay during a half period of oscillation can be estimated as<sup>16</sup>

<sup>16</sup> $\bar{\rho}$  is defined as the energy density in the comoving frame by using the conformally rescaled variables.

$$\begin{aligned} \delta\bar{\rho}_r &= \int_0^{\tau_0/2} d\tau \bar{\Gamma}_\psi \bar{m}_\psi \bar{n}_\psi e^{-\int_0^\tau \bar{\Gamma}_\psi \tau'} \\ &= \frac{1}{8\pi^{3/2} (2\pi^2)^{3/4}} \left(\frac{g_\psi}{\hat{\kappa}_S}\right)^{5/4} Y(f_0, \gamma_\psi), \end{aligned} \quad (57)$$

where  $\gamma_\psi$  and  $Y(f_0, \gamma_\psi)$  are defined by using  $c = 2\pi/\tau_0$  as

$$\begin{aligned} \gamma_\psi &= \frac{c_\psi \mathcal{Y}_\psi^2}{8\pi c} \sqrt{\frac{g_\psi}{\hat{\kappa}_S}}, \\ Y(f_0, \gamma_\psi) &= c\gamma_\psi \int_0^{\tau_0/2} d\tau f_0^2 \sin^2(c f_0 \tau) e^{-2\gamma_\psi \sin^2(\frac{c f_0 \tau}{2})}. \end{aligned} \quad (58)$$

The energy density transferred to the light particles is accumulated at each inflaton zero crossing linearly and its averaged value for  $\tau$  is estimated as

$$\bar{\rho}_r(\tau) = \frac{2\tau}{\tau_0} \delta\bar{\rho}_r = 6.5 \times 10^{-4} \left(\frac{g_\psi}{\hat{\kappa}_S}\right)^{5/4} Y(f_0, \gamma_\psi) \tau, \quad (59)$$

where the substantial change of  $f_0$  is assumed to be negligible during  $\tau$ . Since the total energy density of the inflaton oscillation energy  $\bar{\rho}_\chi$  and the transferred energy  $\bar{\rho}_r$  to light particles is conserved, reheating temperature realized through this process can be estimated from  $\bar{\rho}_{\chi_{\text{end}}} = \bar{\rho}_r$ . It can be written by transferring it to the physical unit as

$$\frac{1}{4\hat{\kappa}_S} \left(\frac{\sqrt{\hat{\kappa}_S \chi_{\text{end}}}}{a}\right)^4 = \frac{\pi^2}{30} g_* T_R^4, \quad (60)$$

where we use  $\bar{\rho}_{\chi_{\text{end}}} = \frac{1}{4\hat{\kappa}_S}$  and  $g_* = 130$ . By applying Eqs. (42) and (59) to this formula, we find<sup>17</sup>

$$T_R = 5.9 \times 10^{15} g_\psi^{5/4} Y(f_0, \gamma_\psi) \text{ GeV}. \quad (61)$$

Since  $h_i \gg h_j$  is satisfied, reheating temperature is expected to be determined by the produced  $\phi$  as long as  $\phi$  is dominantly produced.

If preheating cannot produce relativistic particles effectively, then the dominant energy is still kept in the inflaton oscillation. When the oscillation amplitude of  $\chi$  decreases to be  $O(u)$ , the inflatons start decaying to the light particles through the perturbative processes. Since the mass pattern is expected under the present assumption for the coupling constants in (48) to be

$$2\tilde{m}_\eta < m_\chi < \tilde{M}_D, \tilde{M}_E, \quad (62)$$

the inflaton decay is expected to occur mainly through  $\chi \rightarrow \eta^\dagger \eta$  and  $\chi \rightarrow \phi^\dagger \phi$  at tree level. The decay width of  $\psi(=\phi, \eta)$  is estimated as

<sup>17</sup>The same result can be obtained by using the relation  $H = \frac{1}{2\tau}$  in the radiation dominated era together with Eqs. (42) and (59).

$$\Gamma_\psi \simeq \frac{g_\psi^2}{16\pi\hat{\kappa}_S} m_\chi, \quad (63)$$

where  $g_\psi$  is defined in Eq. (49). After the inflaton decays to  $\eta^\dagger \eta$  and  $\phi^\dagger \phi$ , the SM contents are expected to be thermalized through gauge interactions with  $\eta$  and  $\phi$  immediately. Since  $\Gamma_\psi > H$  is satisfied for  $g_\psi > 10^{-7.1} (\frac{\hat{\kappa}_S}{10^{-8}})^{1/2} (\frac{u}{10^{11} \text{ GeV}})^{1/2}$  at  $\chi \simeq u$ , reheating temperature in such a case can be estimated through  $\frac{1}{4}\hat{\kappa}_S u^4 = \frac{\pi^2}{30} g_* T_R^4$  as<sup>18</sup>

$$T_R \simeq 2.8 \times 10^8 \left(\frac{\hat{\kappa}_S}{10^{-8}}\right)^{1/4} \left(\frac{u}{10^{11} \text{ GeV}}\right) \text{ GeV}, \quad (64)$$

which is independent of  $g_\psi$ . However, if  $\Gamma_\psi > H$  is not satisfied because of a small  $g_\psi$ , the reheating temperature is expected to be determined through  $\Gamma_\psi = H$  and then becomes smaller proportionally to  $g_\psi$ .

In the left panel of Fig. 4, for a case  $\psi = \phi$ , the expected reheating temperature through both processes is plotted as a function  $g_\phi$  in a case  $\tilde{\kappa}_S = 10^{-8}$ ,  $\tilde{\kappa}_\sigma = 10^{-4.5}$ ,  $|\kappa_{\sigma S}|/\tilde{\kappa}_\sigma = 10^{-1.2}$ , and  $u = 10^{11} \text{ GeV}$ . It shows that the reheating temperature is determined by the perturbative process at  $g_\phi < 10^{-6}$ . We also found from the figure that the reheating at  $g_\phi > 10^{-6}$  proceeds through the preheating. Even if the dominant component  $S$  of the inflaton has no coupling with  $\phi$  so that  $g_\phi \simeq |\kappa_{\sigma S}| \kappa_{\phi\sigma} / \tilde{\kappa}_\sigma$ , the preheating is caused by the component  $\sigma$ . It is shown in the right panel where the reheating temperature is plotted for  $\kappa_{\phi\sigma}$  by varying  $|\kappa_{\sigma S}|/\tilde{\kappa}_\sigma$ .<sup>19</sup> These figures show that  $T_R > 2.3 \times 10^8 \text{ GeV}$  can be realized if  $g_\phi > 4 \times 10^{-8}$  is satisfied. However, since the perturbativity of the model is found to be violated at  $g_\phi > 10^{-4.4}$  as mentioned in the previous footnote,  $\kappa_{\phi\sigma} < 10^{-4.4}$  and  $\kappa_{\phi\sigma} < 10^{-2.6}$  should be satisfied, and then the reheating temperature cannot be higher than  $\sim 10^{10} \text{ GeV}$  as found from the figure. Since the decay of  $\phi$  is so effective, it decays soon after their production and much before the inflaton amplitude becomes large during the oscillation. This makes the energy transfer in the preheating inefficient.

In the usual leptogenesis in the seesaw scenario, the right-handed neutrinos are supposed to be thermalized only through the neutrino Yukawa couplings  $h_j$ . In the present

<sup>18</sup>Although a larger value of  $u$  can make the reheating temperature much higher, its upper bound exists. Since a larger  $g_\psi$  is required in that case, it could violate the perturbativity of the model and cause the upper bound for it. For example, if we consider the case with  $y_F = 10^{-1.2}$ , the perturbativity is violated for  $g_\psi > 10^{-4.4}$ . As a result, the reheating temperature due to the perturbative process is bounded as  $T_R < 6.3 \times 10^{13} \text{ GeV}$ .

<sup>19</sup>The condition  $\Gamma_\psi^{-1} < \tau_0/2$  can be confirmed for the parameters used here.

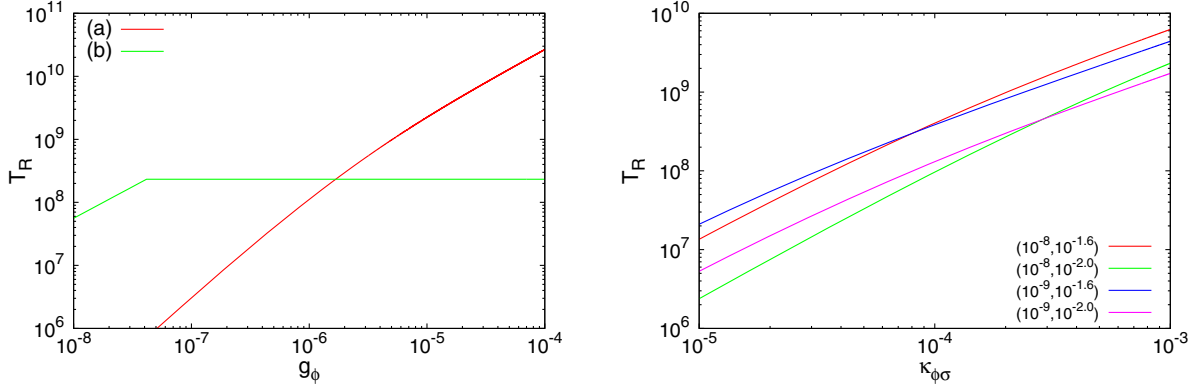


FIG. 4. Left: reheating temperature  $T_R$  (GeV) predicted for both the preheating (a) and the perturbative process (b). They are plotted as a function of  $g_\phi$ . In the case (a), the decay  $\phi \rightarrow \bar{q}t$  is assumed. Right: contribution to the reheating temperature due to a component  $\sigma$  of the inflaton in a case  $\kappa_{\phi S} = 0$ . The reheating temperature  $T_R$  (GeV) is plotted as a function of  $\kappa_{\phi\sigma}$ . Each line represents  $T_R$  for several values of  $(\tilde{\kappa}_S, |\kappa_{\sigma S}|/\tilde{\kappa}_\sigma)$ , where  $\tilde{\kappa}_\sigma$  is fixed at  $10^{-4.5}$  and  $10^{-5.3}$  for  $\tilde{\kappa}_S = 10^{-8}$  and  $10^{-9}$ , respectively.

model, neutrino mass eigenvalues obtained from Eq. (19) require  $h_{2,3} = O(10^{-3})$  to explain the neutrino oscillation data as discussed at a part of Eq. (22). On the other hand, reheating temperature is found to satisfy  $T_R \gtrsim 10^8$  GeV from the above discussion. Since the decay width  $\Gamma_{N_{2,3}}$  of  $N_{2,3}$  and the reheating temperature  $T_R$  satisfy  $\Gamma_{N_{2,3}} > H(T_R)$  and  $T_R > M_{N_{2,3}}$ ,  $N_{2,3}$  are also expected to be in the thermal equilibrium through the inverse decay simultaneously at the reheating period. In the case of  $N_1$ , however, it depends on the magnitude of its Yukawa coupling  $h_1$ , which can be much smaller than others. We should note that  $N_1$  could be effectively generated in the thermal bath, even if  $h_1$  is extremely small, through the scattering of extra fermions that are expected in the thermal equilibrium through gauge interactions in the case  $\tilde{M}_D, \tilde{M}_E < T_R$ . It is a noticeable feature of the present model, which opens a window for low scale leptogenesis.

## IV. PHENOMENOLOGICAL SIGNATURE OF THE MODEL

### A. Leptogenesis

The most interesting feature of this inflation scenario is that thermal leptogenesis could generate sufficient baryon number asymmetry even for  $M_{N_1} < 10^9$  GeV without relying on resonance effect. In the ordinary seesaw framework, neutrino mass is generated as  $(m_\nu)_{\alpha\beta} = \frac{h_{\alpha j} h_{\beta j} \langle \phi \rangle^2}{M_{N_j}}$  through Yukawa interaction  $h_{\alpha j} \bar{\ell}_\alpha \phi N_j$ . Baryon number asymmetry in the Universe [43] is expected to be generated by the same interaction through thermal leptogenesis [44]. If we assume the sufficient lepton asymmetry is generated through the out-of-equilibrium decay of the lightest right-handed neutrino, which has been in the thermal equilibrium, then the reheating temperature  $T_R$  is required to be larger than its mass  $T_R > M_{N_1}$ . Moreover, since it has to be produced sufficiently in the thermal bath, its Yukawa

coupling  $h_{\alpha 1}$  should not be so small. On the other hand, the neutrino mass formula gives a severer upper bound on  $h_{\alpha 1}$  for a smaller  $M_{N_1}$  under the constraints of neutrino oscillation data. These impose a lower bound for  $M_{N_1}$  such as  $10^9$  GeV [45]. This condition for  $M_{N_1}$  is not changed even if  $T_R \gg 10^9$  GeV is satisfied. The problem is caused by such a feature of the model that both the production and the out-of-equilibrium decay of the right-handed neutrino have to be caused only by the same neutrino Yukawa coupling. It does not change in the original scotogenic model either [32]. In that model, the right-handed neutrino mass can be much smaller than  $10^9$  GeV, keeping the neutrino Yukawa couplings to be rather larger values by fixing  $|\lambda_5|$  at a smaller value in a consistent way with the neutrino oscillation data. However, the washout of the generated lepton number due to the inverse decay of the right-handed neutrinos becomes so effective in that case. As a result, successful leptogenesis cannot be realized for a lighter right-handed neutrino than  $10^8$  GeV.<sup>20</sup> It is a notable aspect in the present model that this situation can be changed by the particles which are introduced to explain the  $CP$  issues in the SM.

We note that the interaction between the right-handed neutrino  $N_1$  and extra vectorlike fermions  $F$  mediated by  $\tilde{\sigma}$  could change the situation.<sup>21</sup> The lightest right-handed neutrino  $N_1$  can be effectively produced in the thermal bath through the extra fermions scattering  $\bar{D}_L D_R, \bar{E}_L E_R \rightarrow N_1 N_1$  mediated by  $\tilde{\sigma}$  if  $D_{L,R}$  and/or  $E_{L,R}$  are in the thermal equilibrium at a certain temperature  $T$ . In that case, both conditions  $T > \tilde{M}_F, M_{N_1}$  and  $\Gamma_{FF} \simeq H(T)$  are required to

<sup>20</sup>Low scale leptogenesis in the scotogenic model has been studied intensively in [46]. However, the lightest right-handed neutrino is assumed to be in the thermal equilibrium initially there.

<sup>21</sup>The similar mechanism has been discussed in models with a different type of inflaton [33,47].

be satisfied, where  $\Gamma_{FF}$  is the reaction rate of this scattering. Mass of these fermions is determined by the VEVs  $u$  and  $w$ , which should be larger than the lower bound of PQ symmetry breaking scale. Since the rough estimation of  $\Gamma_{FF} \simeq H(T)$  for relativistic  $F$  and  $N_1$  gives

$$T \simeq 5.8 \times 10^8 \left( \frac{y_F}{10^{-1.2}} \right)^2 \left( \frac{y_{N_1}}{10^{-2}} \right)^2 \text{ GeV}, \quad (65)$$

we find that  $T > \tilde{M}_F$ ,  $M_{N_1}$  could be satisfied for suitable values of  $y_F$  and  $y_{N_1}$ . It is crucial that this does not depend on the magnitude of the  $N_1$  Yukawa coupling  $h_1$ . If an extremely small value is assumed for  $h_1$ , successful

leptogenesis is allowed in a consistent way with neutrino oscillation data even for  $M_{N_1} < 10^9$  GeV.

After  $N_1$  is produced in the thermal bath through the scattering of the extra fermions mediated by  $\tilde{\sigma}$ , it is expected to decay to  $\ell_\alpha \eta^\dagger$  by a strongly suppressed Yukawa coupling. Since its substantial decay occurs after the washout processes are frozen out, the generated lepton number asymmetry can be efficiently converted to the baryon number asymmetry through sphaleron processes. This scenario can be checked by solving Boltzmann equations for  $Y_{N_1}$  and  $Y_L (\equiv Y_\ell - Y_{\bar{\ell}})$ , where  $Y_\psi$  is defined as  $Y_\psi = \frac{n_\psi}{s}$  by using the  $\psi$  number density  $n_\psi$  and the entropy density  $s$ . Boltzmann equations analyzed here are given as

$$\begin{aligned} \frac{dY_{N_1}}{dz} &= -\frac{z}{sH(M_{N_1})} \left( \frac{Y_{N_1}}{Y_{N_1}^{\text{eq}}} - 1 \right) \left[ \gamma_D^{N_1} + \left( \frac{Y_{N_1}}{Y_{N_1}^{\text{eq}}} + 1 \right) \sum_{F=D,E} \gamma_F \right], \\ \frac{dY_L}{dz} &= -\frac{z}{sH(M_{N_1})} \left[ \varepsilon \left( \frac{Y_{N_1}}{Y_{N_1}^{\text{eq}}} - 1 \right) \gamma_D^{N_1} - \frac{2Y_L}{Y_\ell^{\text{eq}}} \sum_{j=1,2,3} \left( \frac{\gamma_D^{N_j}}{4} + \gamma_{N_j} \right) \right], \end{aligned} \quad (66)$$

where  $z = \frac{M_{N_1}}{T}$  and an equilibrium value of  $Y_\psi$  is represented by  $Y_\psi^{\text{eq}}$ .  $H(T)$  is the Hubble parameter at temperature  $T$  and the  $CP$  asymmetry  $\varepsilon$  for the decay of  $N_1$  is expressed as

$$\begin{aligned} \varepsilon &= \frac{1}{8\pi} \sum_{j=2,3} \frac{\text{Im}[\sum_\alpha (\tilde{h}_{\alpha 1} \tilde{h}_{\alpha j}^*)]^2}{\sum_\alpha \tilde{h}_{\alpha 1} \tilde{h}_{\alpha 1}^*} F \left( \frac{M_{N_j}^2}{M_{N_1}^2} \right), \\ &= \frac{1}{16\pi} \left[ 4|h_2|^2 F \left( \frac{y_{N_2}^2}{y_{N_1}^2} \right) \sin 2(\theta_1 - \theta_2) + |h_3|^2 F \left( \frac{y_{N_3}^2}{y_{N_1}^2} \right) \sin 2(\theta_1 - \theta_3) \right], \end{aligned} \quad (67)$$

where  $h_j = |h_j| e^{i\theta_j}$  and  $F(x) = \sqrt{x} [1 - (1+x) \ln \frac{1+x}{x}]$ . A reaction density for the decay  $N_j \rightarrow \ell_\alpha \eta^\dagger$  and for the lepton number violating scattering mediated by  $N_j$  is expressed by  $\gamma_D^{N_j}$  and  $\gamma_{N_j}$ , respectively [32].  $\gamma_F$  represents a reaction density for the scattering  $\bar{D}_L D_R, \bar{E}_L E_R \rightarrow N_1 N_1$ . We assume that  $(D_L, D_R)$  and  $(E_L, E_R)$  are in the thermal equilibrium and  $Y_{N_1} = Y_L = 0$  at  $z = z_R (\equiv \frac{M_{N_1}}{T_R})$ .

Now we fix the model parameters for numerical study of Eq. (66) by taking account of the discussion in the previous part. We consider two cases for the VEVs of the singlet scalars such that

$$\begin{aligned} \text{(I)} \quad & w = 10^9 \text{ GeV}, \quad u = 10^{11} \text{ GeV}, \\ \text{(II)} \quad & w = 10^{11} \text{ GeV}, \quad u = 10^{13} \text{ GeV}, \end{aligned} \quad (68)$$

where the axion could be a dominant DM in case (II). The parameters  $\tilde{\kappa}_S$ ,  $\tilde{\kappa}_\sigma$ , and  $\kappa_{\sigma S}$ , which characterize the inflaton  $\chi$ , are fixed to  $\tilde{\kappa}_S = 10^{-8}$ ,  $\tilde{\kappa}_\sigma = 10^{-4.5}$ , and  $|\kappa_{\sigma S}| = 10^{-6.1}$ . These are used in the right panel of Fig. 4. The condition  $\mathcal{F}_f \mathcal{F}_f^\dagger > \mu_F^2$  for which the  $CP$  phases in the CKM and PMNS matrices can be generated is reformulated as  $\delta \equiv \tilde{M}_F / \mu_F > \sqrt{2}$ . If we confine our study on a case  $y_f = (0, 0, y)$  and  $\tilde{y}_f = (0, \tilde{y}, 0)$  for simplicity,<sup>22</sup> then we have a relation  $y^2 + \tilde{y}^2 = (\delta^2 - 1) \frac{w^2}{u^2} y_F^2$  among Yukawa couplings of the extra fermions. We fix them as  $\delta = \sqrt{3}$ ,  $\tilde{y}/y = 0.5$  and  $y_D = y_E = 10^{-1.2}$  at the scale  $\tilde{M}$ . Parameters relevant to the neutrino mass generation are fixed as

$$\begin{aligned} y_{N_2} &= 2 \times 10^{-2}, \quad y_{N_3} = 4 \times 10^{-2} \quad \text{for (I) and (II),} \\ y_{N_1} &= 7 \times 10^{-3}, \quad |h_1| = 6 \times 10^{-7} \quad |\tilde{\lambda}_5| = 10^{-3}, \quad M_\eta = 1 \text{ TeV} \quad \text{for (I),} \\ y_{N_1} &= 10^{-3}, \quad |h_1| = 6 \times 10^{-5}, \quad |\tilde{\lambda}_5| = 5 \times 10^{-3}, \quad M_\eta = 0.9 \text{ TeV} \quad \text{for (II).} \end{aligned} \quad (69)$$

<sup>22</sup>It is considered as an example in Appendix A.

These parameters fix the mass of relevant particles as

$$\begin{aligned}
 \text{(I)} \quad & M_{N_1} = 7 \times 10^6 \text{ GeV}, \quad M_{N_2} = 2 \times 10^7 \text{ GeV}, \quad M_{N_3} = 4 \times 10^7 \text{ GeV}, \\
 & \tilde{M}_D = \tilde{M}_E = 1.1 \times 10^8 \text{ GeV}, \quad m_{\tilde{\sigma}} = 8 \times 10^6 \text{ GeV}, \\
 \text{(II)} \quad & M_{N_1} = 10^8 \text{ GeV}, \quad M_{N_2} = 2 \times 10^9 \text{ GeV}, \quad M_{N_3} = 4 \times 10^9 \text{ GeV}, \\
 & \tilde{M}_D = \tilde{M}_E = 1.1 \times 10^{10} \text{ GeV}, \quad m_{\tilde{\sigma}} = 8 \times 10^8 \text{ GeV}.
 \end{aligned} \tag{70}$$

Although the mediator has a small component  $\tilde{S}$ , it can be safely treated as  $\tilde{\sigma}$ . For these parameters, the  $CP$  asymmetry  $\varepsilon$  in the  $N_1$  decay takes a value of  $O(10^{-6})$  in both cases if the maximum  $CP$  phase is assumed. DM is determined by the couplings  $\tilde{\lambda}_3$  and  $\lambda_4$ . Since they are fixed so as to realize the correct DM abundance by the neutral component of  $\eta$  in the case (I), it cannot saturate the required DM abundance for the same  $\tilde{\lambda}_3$  and  $\lambda_4$  in the case (II) as found from Fig. 1. The axion could be a dominant component of DM in the case (II) since  $w$  is taken to be a sufficient value for it.

We give a remark on these couplings here. It is crucial to examine whether the above parameters used in this analysis are consistent with the potential stability conditions (5), (17) and also the perturbativity of the model under constraints coming from the requirements for the DM relic abundance and the reheating temperature. If DM relic abundance is realized by the neutral component of  $\eta$ , both  $\tilde{\lambda}_3$  and  $\lambda_4$  should take values shown in Fig. 1. On the other hand, the reheating temperature required for sufficient leptogenesis can be realized for  $\kappa_{\phi\sigma} \gtrsim 10^{-4}$  or  $\kappa_{\phi S} \gtrsim 10^{-7}$  as found from the analysis of the reheating temperature. Since they can give rather large contributions to the  $\beta$  functions of the scalar quartic couplings  $\kappa_{\eta\sigma}$  and  $\kappa_{\eta S}$  for example, the perturbativity up to the inflation scale could be violated. An upper bound on  $g_\phi$  has to be imposed to escape it and it results in an upper bound on the reheating

temperature discussed already. The parameter sets used here have been confirmed to satisfy these conditions through the RGEs study. Details of the used parameters in the analysis are addressed in Appendix B and an example of the results of this study is presented in the right panel of Fig. 1.

Solutions of the Boltzmann equations in the cases (I) and (II) are shown in Fig. 5. The lightest right-handed neutrino mass in each case is  $M_{N_1} = 7 \times 10^6$  and  $10^8$  GeV. In both cases, the sufficient baryon number asymmetry is found to be produced. The figure for the case (I) shows clearly that the present scenario works well.  $Y_{N_1}$  reaches a value near  $Y_{N_1}^{\text{eq}}$  through the scattering of the extra fermions as expected. Substantial out-of-equilibrium decay occurs at  $z > 10$  to generate the lepton number asymmetry. The delay of the decay due to the small  $h_1$  could make the washout of the lepton number asymmetry ineffective. On the other hand, we cannot definitely find a signature of the scenario in the case (II), where the  $N_1$  mass is near the bound for which the usual leptogenesis can generate the required baryon number asymmetry in the original scotogenic model [32]. The figure shows that additional contribution to the  $N_1$  production starts at  $z \simeq 0.1$ . It is considered to be brought about by the  $N_1$  inverse decay since it is expected to become effective around  $z \sim (\frac{6.3 \times 10^{-5}}{h_1}) (\frac{M_{N_1}}{10^8 \text{ GeV}})$ . The figure shows that it plays a

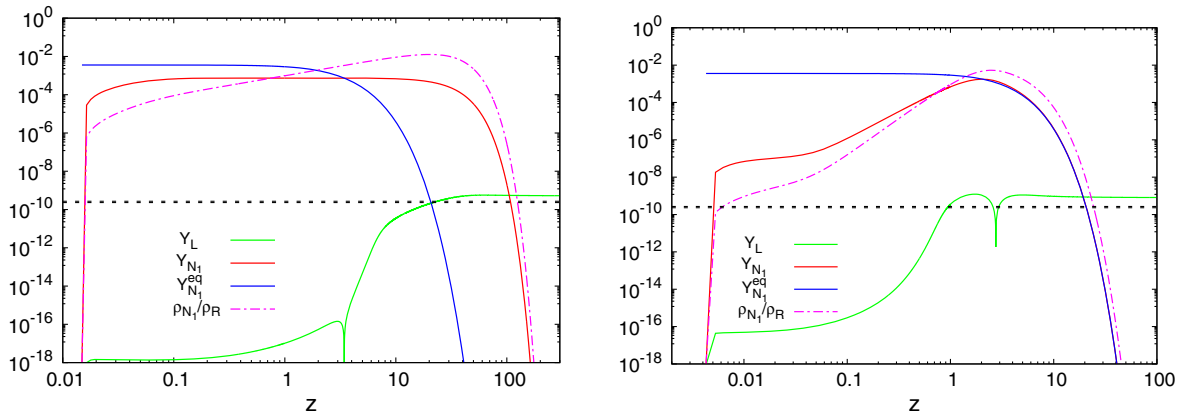


FIG. 5. Evolution of  $Y_{N_1}$  and  $Y_L$  obtained as solutions of Boltzmann equations. Results of the case (I) is shown in the left panel for  $\kappa_{\phi\sigma} = 10^{-4}$  and  $\kappa_{\phi S} = \kappa_{\eta S} = 0$ . Results of the case (II) is shown in the right panel for  $\kappa_{\phi S} = \kappa_{\eta S} = 10^{-6}$  and  $\kappa_{\phi\sigma} = \kappa_{\eta\sigma} = 0$ . Other parameters in each case are given in the text. Initial values for them are fixed as  $Y_{N_1} = Y_L = 0$  at  $z = z_R$ .  $\rho_{N_1}/\rho_R$  represents a ratio of the energy density of  $N_1$  to the one of radiation.



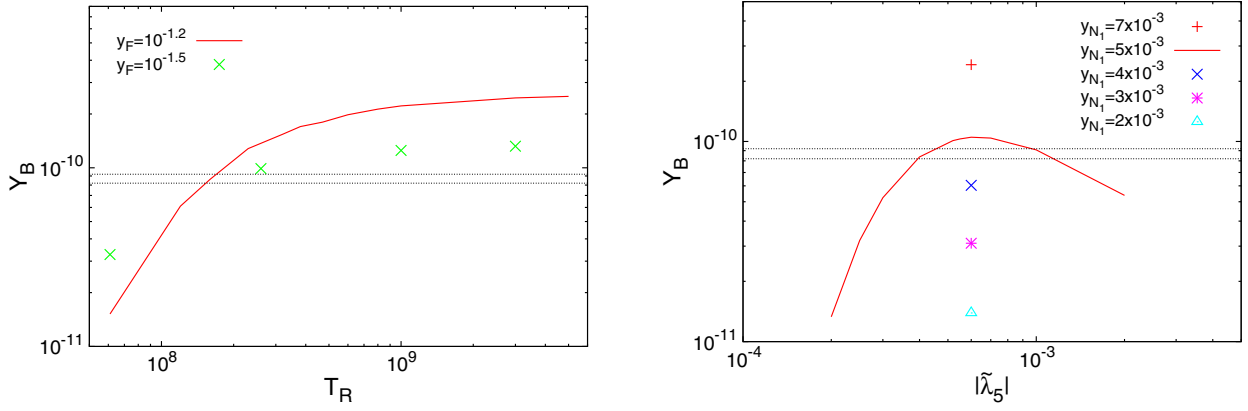


FIG. 6. Left: baryon number asymmetry generated at the expected reheating temperature  $T_R$  (GeV) in the case (I). It is plotted by a red solid line for  $y_D = 10^{-1.2}$  and by green crosses for  $y_D = 10^{-1.5}$ . Right: baryon number asymmetry generated at  $T_R = 10^9$  GeV for various values of  $\tilde{\lambda}_5$  and  $y_{N_1}$  in the case (I). In both panels, other parameters are fixed at the ones given in (69).

main role for the  $N_1$  production. As a result, the leptogenesis in this case results in the ordinary one where the lower mass bound of  $N_1$  is  $O(10^8)$  GeV.

These results show that the model with suitable parameters can generate a sufficient amount of baryon number asymmetry through leptogenesis even if the reheating temperature is lower than  $10^9$  GeV as long as  $M_{N_1} < T_R$  GeV is satisfied. In the present model, both the right-handed neutrino mass and the extra fermion mass are determined by  $M_{N_j} = y_{N_j} w$  and  $\tilde{M}_F = \delta y_F w$ . Since  $w$  is fixed as the  $PQ$  symmetry breaking scale and  $\delta > 1$  is imposed for the realization of the substantial  $CP$  phases in the CKM and PMNS matrices, their mass cannot be arbitrarily smaller than  $10^9$  GeV under the condition that the scattering of the extra fermions to the right-handed neutrinos is effective. Because of this reason, low scale leptogenesis, which can be a distinguishable feature of the model, tends to be allowed only for the case where the  $PQ$  symmetry breaking occurs at a neighborhood of its lower bound. Even in that case, successful leptogenesis is expected to be realized only in the range  $M_{N_1} > 4 \times 10^6 (\frac{y_F}{10^{-1.2}})^{-1/2}$  GeV for the case  $T_R > 10^8$  GeV since  $T$  in Eq. (65) should satisfy  $T > \tilde{M}_F, M_{N_1}$  for the sufficient  $N_1$  production.

In Fig. 6, we show the baryon number asymmetry  $Y_B$  generated in the case (I) varying the values of relevant parameters. In the left panel,  $Y_B$  is plotted as a function of the reheating temperature, which is fixed by the inflaton composition and its coupling with  $\phi$  and  $\eta$ . Two values of  $y_F$  are used in this plot. The  $N_1$  production in the present scenario depends on the reheating temperature and the couplings  $y_F, y_{N_1}$ . A red solid line representing  $Y_B$  is expected for the parameters given in Eq. (69) for the case (I). It becomes larger and reaches an upper bound  $Y_B \simeq 2.5 \times 10^{-10}$  when the reheating temperature increases to  $10^{10}$  GeV. This behavior can be understood if we take

into account that the equilibrium number density of extra fermions are suppressed by the Boltzmann factor at lower reheating temperature and then the  $N_1$  production due to the scattering of extra fermions is suppressed. We also plot  $Y_B$  for a smaller value of  $y_F$  by green crosses at some typical  $T_R$ . They show that  $Y_B$  takes smaller values for a smaller  $y_F$  since the  $N_1$  production cross section is proportional to  $y_F^2$ .<sup>23</sup> In the right panel,  $Y_B$  is plotted by varying  $|\tilde{\lambda}_5|$  and  $y_{N_1}$ . A red solid line represents it as a function of  $|\tilde{\lambda}_5|$  for a fixed  $y_{N_1} = 5 \times 10^{-3}$ . Since the neutrino oscillation data have to be imposed on Eq. (21), Yukawa couplings  $h_{2,3}$  are settled by  $|\tilde{\lambda}_5|, y_{N_2}$  and  $y_{N_3}$ . The  $CP$  asymmetry  $\varepsilon$  and the washout of the generated lepton number asymmetry are mainly determined by  $h_{2,3}$  for the fixed  $y_{N_2}$  and  $y_{N_3}$  as found from Eq. (67). Since a smaller  $|\tilde{\lambda}_5|$  makes  $h_{2,3}$  larger and then both  $\varepsilon$  and washout larger,  $Y_B$  takes a maximum value for a certain  $|\tilde{\lambda}_5|$ , which is found in the figure. We also plot  $Y_B$  by varying  $y_{N_1}$  for a fixed  $|\tilde{\lambda}_5|$  in the same panel. A smaller  $y_{N_1}$  makes the  $N_1$  production less effective for a fixed  $y_F$  and then its lower bound is expected to appear for successful leptogenesis. It gives the lower bound of  $M_{N_1}$  as  $\sim 4 \times 10^6$  GeV as predicted above.

Although other parameters are fixed at the ones given in (69) in these figures, it is useful to give remarks on their dependence here. If  $\delta$  takes a larger value, then the mass of extra fermions  $\tilde{M}_F$  becomes larger to suppress the reaction density  $\gamma_F$  due to the Boltzmann factor. As a result, the  $N_1$  number density generated through the scattering becomes smaller and the resulting  $Y_B$  also becomes smaller. If  $h_1$  is much smaller, then  $N_1$  decay delays and the entropy

<sup>23</sup>Since the effect of Boltzmann suppression caused by its mass  $\tilde{M}_F = \delta y_F w$  could be dominant at lower  $T_R$  compared with the effect on the cross section, the smaller  $y_F$  gives a larger  $Y_B$  at  $T_R < 10^8$  GeV in this case.

produced through the decay of relic  $N_1$  might dilute the generated lepton number asymmetry.

### B. Dark matter and isocurvature fluctuations

This model has two DM candidates. One is the lightest neutral component of  $\eta$  with  $Z_2$  odd parity which is an indispensable ingredient of the model. It is known to be a good DM candidate which does not cause any contradiction with known experimental data as long as its mass is in the TeV range where the coannihilation can be effective [32,48,49]. As found from Fig. 1, both the DM abundance and the DM direct search bound can be satisfied if the couplings  $\tilde{\lambda}_3$  and  $|\lambda_4|$  take suitable values of  $O(1)$ . Although these parameters could affect the perturbativity of the scalar quartic couplings through the radiative corrections, we can safely escape such problems in certain parameter regions. The results obtained for the case (I) in the previous part are derived by supposing that the required DM is  $\eta_R$ .

Axion is another promising candidate in the model. However, the axion could be a dominant component of DM only for  $f_a \sim 10^{11}$  GeV although it depends on the contribution from the axion string decay [50]. We consider the case (II) as such an example. As described before, the PQ symmetry is spontaneously broken during the inflation since the inflaton contains the radial component of  $\sigma$ . As a result, the axion appears as the phase  $\theta$  of  $\sigma$ . Since the axion potential is flat during the inflation, the axion gets a quantum fluctuation  $\delta A = (H/2\pi)^2$  and it can cause isocurvature fluctuation in the CMB amplitude [51,52]. A canonically normalized axion  $A$  is defined by noting Eq. (26) as

$$\frac{\partial A}{\partial \theta} = \frac{\tilde{\sigma}}{\Omega^2} \sqrt{\Omega^2 + 6\tilde{\xi}_\sigma \frac{\tilde{\sigma}^2}{M_{\text{pl}}^2}} \simeq \frac{\sqrt{\chi} M_{\text{pl}} |\kappa_{\sigma S}|}{\tilde{\xi}_S^{1/4} \tilde{\kappa}_\sigma} \equiv \chi_{\text{iso}}. \quad (71)$$

Since the axion interacts with other fields very weakly, it causes the isocurvature fluctuation as the fluctuation of its number density  $n_A$ . The amplitude of its power spectrum can be expressed as

$$\mathcal{P}_i(k) = \left\langle \left| \frac{\delta n_A}{n_A} \right|^2 \right\rangle = \frac{H_k^2}{\pi^2 \chi_{\text{iso}}^2 \langle \theta^2 \rangle}. \quad (72)$$

Since the axion is only a source of the isocurvature fluctuation in this model, its fraction in the power spectrum is given as

$$\alpha = \frac{R_a^2 \mathcal{P}_i(k)}{R_a^2 \mathcal{P}_i(k) + \mathcal{P}_s(k)} \simeq 8\tilde{\epsilon}_{\tilde{\xi}_S}^{1/2} \frac{M_{\text{pl}} R_a^2}{\chi_k \langle \theta^2 \rangle} \left( \frac{\tilde{\kappa}_\sigma}{\kappa_{\sigma S}} \right)^2, \quad (73)$$

where  $\mathcal{P}_s(k) = A_s$ , which is given in Eq. (38).  $R_a$  is a fraction of the axion energy density in the CDM and defined as  $R_a = \Omega_a / \Omega_{\text{CDM}}$ . If we use a relation [53]

$$R_a = \frac{\langle \theta^2 \rangle}{6 \times 10^{-6}} \left( \frac{f_a}{10^{16} \text{ GeV}} \right)^{7/6}, \quad (74)$$

then we find

$$\alpha = 3.25 \times 10^{-5} \tilde{\xi}_S^{1/2} \frac{M_{\text{pl}}}{\chi_k} \left( \frac{55}{\mathcal{N}_k} \right)^2 \left( \frac{f_a}{10^{10} \text{ GeV}} \right)^{7/6} R_a \left( \frac{\tilde{\kappa}_\sigma}{\kappa_{\sigma S}} \right)^2. \quad (75)$$

Since the Planck data constrain  $\alpha$  as  $\alpha \leq 0.037$  at  $k = 0.05 \text{ Mpc}^{-1}$  [15], we have a condition for the model to be consistent with the present observation of the isocurvature fluctuation in the CMB as

$$R_a < \frac{67}{\tilde{\xi}_S^{1/2} M_{\text{pl}}} \left( \frac{\mathcal{N}_k}{55} \right)^2 \left( \frac{10^{11} \text{ GeV}}{w} \right)^{7/6} \left( \frac{\kappa_{\sigma S}}{\tilde{\kappa}_\sigma} \right)^2, \quad (76)$$

where  $f_a = w$  is used. In the case (I), this gives no constraint and the parameters used in the present study to estimate the reheating temperature in Fig. 4 and the baryon number asymmetry are consistent with the observational data. DM can be identified with the neutral component of  $\eta$ . On the other hand, in the case (II), the isocurvature condition can be satisfied for  $R_a < 0.21$  if  $|\kappa_{\sigma S}|/\tilde{\kappa}_\sigma = 10^{-1.6}$  is assumed and for  $R_a < 0.034$  if  $|\kappa_{\sigma S}|/\tilde{\kappa}_\sigma = 10^{-2}$  is assumed. The isocurvature constraint forbids the axion to be a dominant DM component, and the neutral component of  $\eta$  is required to play a role of the dominant DM in this case also.

## V. SUMMARY

We have proposed a model that could give an explanation for the origin of the  $CP$  phases in both the CKM and PMNS matrices and the strong  $CP$  problem. It is a simple extension of the SM with vectorlike extra fermions and several scalars. In order to control the couplings of new fields, global symmetry is imposed. If the  $CP$  symmetry is spontaneously broken in a singlet scalar sector at an intermediate scale, then it can be transformed to the CKM and PMNS matrices through the mixing between the extra fermions and the ordinary quarks or the charged leptons. On the other hand, since the colored extra fermions play the same role as the ones in the KSVZ model for the strong  $CP$  problem, the strong  $CP$  problem could be solved through the PQ mechanism. After the symmetry breaking due to the singlet scalars, the leptonic sector of the model is reduced to the scotogenic model, which can explain the small neutrino masses and the DM abundance due to the remnant discrete symmetry of the imposed symmetry. Singlet scalars introduced to explain the  $CP$  issues can play a role of inflaton if it has a nonminimal coupling with the Ricci scalar. We suppose this coupling is of order one. In that case, although it gives the similar prediction for the scalar spectral index and the tensor to scalar ratio to the one

of the Higgs inflation, reheating phenomena is different from it since the radiation domination starts just after the end of inflation.

The model has a notable phenomenological feature in addition to these. The extra fermions that are introduced for the  $CP$  issues could make the thermal leptogenesis generate the sufficient baryon number asymmetry even if the lightest right-handed neutrino mass is much lower than  $10^9$  GeV, which is the well-known lower bound of the right-handed neutrino mass for successful leptogenesis in the ordinary seesaw scenario. Although the model allows low scale leptogenesis, it is difficult to distinguish it from other thermal leptogenesis model experimentally. However, if we consider its supersymmetric extension, it could give a possibility to escape the gravitino problem. The model is constrained by the isocurvature fluctuation which is caused by the spontaneous breaking of the PQ symmetry during the inflation. We find that its present observation can be consistent with the model even if the DM relic abundance is imposed on the model. Although the relic density of axion should be a small fraction of the DM, there is a neutral component of the inert doublet scalar as an alternative candidate of DM in the model. It can explain the DM abundance just as in the scotogenic model without affecting other predictions of the model. It is remarkable that the model has potentiality to explain various issues in the SM although the model is rather simple. It may deserve further study.

### ACKNOWLEDGMENTS

This work is partially supported by a Grant-in-Aid for Scientific Research (C) from Japan Society for Promotion of Science (Grant No. 18K03644). N. S. R is supported by *Program 5000 Doktor* under Ministry of Religious Affairs (MORA), Republic of Indonesia.

### APPENDIX A: A SIMPLE EXAMPLE FOR $A_f$

In this Appendix, we present a simple example that could bring about a phase in the CKM matrix. In this example, we assume  $w = 10^9$  GeV and  $u = 10^{11}$  GeV, and also the relevant Yukawa couplings  $h_d$ ,  $y_d$ , and  $\tilde{y}_d$  to be written by using real constant parameters as

$$h_d = c \begin{pmatrix} \epsilon^4 & \epsilon^3 & p_1 \epsilon^3 \\ \epsilon^3 & \epsilon^2 & p_2 \epsilon^2 \\ \epsilon^2 & p_3 & -p_3 \end{pmatrix}, \quad y_d = (0, y, 0), \quad \tilde{y}_d = (0, 0, \tilde{y}). \quad (\text{A1})$$

As long as  $\epsilon$  satisfies  $\epsilon < 1$ , the down type quark mass matrix  $m_d (\equiv h_d \langle \tilde{\phi} \rangle)$  has hierarchical mass eigenvalues. Here, we introduce  $X_{ij}$  and  $Y_{ij}$  whose definition is given as

$$X_{ij} = 1 + p_i p_j + \frac{y^2 + \tilde{y}^2 p_i p_j + y \tilde{y} (p_i + p_j) \cos 2\rho}{y^2 + \tilde{y}^2} \left(1 - \frac{1}{\delta^2}\right),$$

$$Y_{ij} = \frac{y \tilde{y} (p_i - p_j) \sin 2\rho}{y^2 + \tilde{y}^2} \left(1 - \frac{1}{\delta^2}\right), \quad (\text{A2})$$

where  $\delta$  is defined as  $\delta = \tilde{M}_F / \mu_F$ . If we define  $R_{ij}$  and  $\theta_{ij}$  by using these quantities as

$$R_{ij} = \sqrt{X_{ij}^2 + Y_{ij}^2}, \quad \tan \theta_{ij} = \frac{Y_{ij}}{X_{ij}}, \quad (\text{A3})$$

then the component of Eq. (13) is found to be expressed under the assumption  $\mu_D^2 < \mathcal{F}_d \mathcal{F}_d^\dagger$  as

$$(A_d^{-1} m^2 A_d)_{ij} = c^2 \langle \tilde{\phi} \rangle^2 \epsilon_{ij} R_{ij} e^{i\theta_{ij}}, \quad (\text{A4})$$

where  $\epsilon_{ij}$  is defined as

$$\epsilon_{11} = \epsilon^6, \quad \epsilon_{22} = \epsilon^4, \quad \epsilon_{33} = 1, \quad \epsilon_{12} = \epsilon_{21} = \epsilon^5,$$

$$\epsilon_{13} = \epsilon_{31} = \epsilon^3, \quad \epsilon_{23} = \epsilon_{32} = \epsilon^2. \quad (\text{A5})$$

By solving Eq. (A4), we find that  $A_d$  is approximately written as

$$A_d \simeq \begin{pmatrix} 1 & -\lambda & \lambda^3 \left( \frac{X_{23}}{|\alpha|^2 X_{33}} e^{i\vartheta} - \frac{X_{13}}{|\alpha|^3 X_{33}} \right) \\ \lambda & 1 & -\lambda^2 \frac{X_{23}}{|\alpha|^2 X_{33}} e^{i\vartheta} \\ \lambda^3 \frac{X_{13}}{|\alpha|^3 X_{33}} & \lambda^2 \frac{X_{23}}{|\alpha|^2 X_{33}} e^{-i\vartheta} & 1 \end{pmatrix}, \quad (\text{A6})$$

where the constants  $\lambda$ ,  $\alpha$ , and  $\vartheta$  are defined by

$$\alpha = \frac{X_{12} X_{33} - X_{13} X_{23} e^{-i(\theta_{23} + \theta_{12} - \theta_{13})}}{X_{22} X_{33} - X_{23}^2}, \quad \lambda = |\alpha| \epsilon,$$

$$\vartheta = \arg(\alpha) + \theta_{23} + \theta_{12} - \theta_{13}. \quad (\text{A7})$$

This expression shows that  $A_d$  could have a nontrivial phase that gives the origin of the CKM phase. If the diagonalization matrix  $O^L$  for a mass matrix of the up type quarks takes an almost diagonal form, the CKM matrix could be obtained as  $V_{\text{CKM}} \simeq A_d$ . As an example, if we assume  $\cos \rho = \frac{\pi}{4}$  and fix other parameters as

$$y_F = 10^{-1.5}, \quad \delta = \sqrt{3}, \quad y = 4 \times 10^{-4}, \quad \tilde{y} = 2 \times 10^{-4},$$

$$p_1 = 1.1, \quad p_2 = -0.9, \quad p_3 = 1, \quad \epsilon = 0.2, \quad c = 0.014, \quad (\text{A8})$$

then we obtain  $\lambda = 0.22$  and the Jarlskog invariant [54] as  $J (\equiv \text{Im}[A_{12} A_{13}^* A_{23} A_{22}^*]) = -1.6 \times 10^{-6}$ . The mass eigenvalues for the down type quarks are obtained as

$$\begin{aligned}
m_d &= \left\{ X_{11} - \frac{X_{13}^2}{X_{33}} + |\alpha|^2 \left( X_{22} - \frac{X_{23}^2}{X_{33}} - 2 \right) \right\}^{1/2} \epsilon^3 c \langle \tilde{\phi} \rangle \\
&\simeq 3.3 \text{ MeV}, \\
m_s &= \left( X_{22} - \frac{X_{23}^2}{X_{33}} \right)^{1/2} \epsilon^2 c \langle \tilde{\phi} \rangle \simeq 138 \text{ MeV}, \\
m_b &= X_{33}^{1/2} c \langle \tilde{\phi} \rangle \simeq 4.2 \text{ GeV}. \tag{A9}
\end{aligned}$$

Although a diagonalization matrix  $A_e$  for the charged lepton sector may be considered to take the same form as  $A_d$ , it is not favorable for a large  $CP$  phase in the PMNS matrix. In that case, since  $A_e$  is the nearly diagonal, large flavor mixing has to be caused only by the neutrino sector

and the Dirac  $CP$  phase in the PMNS matrix becomes small as a result. A large  $CP$  phase in the PMNS matrix requires  $A_e$  to have rather large off-diagonal elements also.

## APPENDIX B: RGEs FOR COUPLING CONSTANTS

In order to examine both the stability and the perturbativity of the model from the weak scale to the Planck scale, we have to know the running of the coupling constants in Eq. (1). If we fix these coupling constants at an intermediate scale and solve the RGEs to the Planck scale, then we can find their values throughout the scale. The one-loop RGEs of the relevant coupling constants are given as

$$\begin{aligned}
16\pi^2 \mu \frac{\partial \lambda_1}{\partial \mu} &= 24\lambda_1^2 + \lambda_3^2 + (\lambda_3 + \lambda_4)^2 + \kappa_{\phi\sigma}^2 + \kappa_{\phi S}^2 + \frac{3}{8}(3g^4 + g^4 + 2g^2g^2) - 3\lambda_1(3g^2 + g^2 - 4h_t^2) - 6h_t^4, \\
16\pi^2 \mu \frac{\partial \lambda_2}{\partial \mu} &= 24\lambda_2^2 + \lambda_3^2 + (\lambda_3 + \lambda_4)^2 + \kappa_{\eta\sigma}^2 + \kappa_{\eta S}^2 + \frac{3}{8}(3g^4 + g^4 + 2g^2g^2) \\
&\quad - 3\lambda_2(3g^2 + g^2) + 4\lambda_2(2h_2^2 + 3h_3^2) - 8h_2^4 - 18h_3^4, \\
16\pi^2 \mu \frac{\partial \lambda_3}{\partial \mu} &= 2(\lambda_1 + \lambda_2)(6\lambda_3 + 2\lambda_4) + 4\lambda_3^2 + 2\lambda_4^2 + 2\kappa_{\phi\sigma}\kappa_{\eta\sigma} + 2\kappa_{\phi S}\kappa_{\eta S} \\
&\quad + \frac{3}{4}(3g^4 + g^4 - 2g^2g^2) - 3\lambda_3(3g^2 + g^2) + 2\lambda_3(3h_t^2 + 2h_2^2 + 3h_3^2), \\
16\pi^2 \mu \frac{\partial \lambda_4}{\partial \mu} &= 4(\lambda_1 + \lambda_2)\lambda_4 + 8\lambda_3\lambda_4 + 4\lambda_4^2 + 3g^2g^2 - 3\lambda_4(3g^2 + g^2) + 2\lambda_4(3h_t^2 + 2h_2^2 + 3h_3^2), \\
16\pi^2 \mu \frac{\partial \kappa_S}{\partial \mu} &= 20\kappa_S^2 + \kappa_{\sigma S}^2 + 2(\kappa_{\phi S}^2 + \kappa_{\eta S}^2) + 4\kappa_S[3(y_d^2 + \tilde{y}_d^2) + y_e^2 + \tilde{y}_e^2] - 2[3(y_d^2 + \tilde{y}_d^2)^2 + (y_e^2 + \tilde{y}_e^2)^2], \\
16\pi^2 \mu \frac{\partial \kappa_\sigma}{\partial \mu} &= 20\kappa_\sigma^2 + \kappa_{\sigma S}^2 + 2(\kappa_{\phi\sigma}^2 + \kappa_{\eta\sigma}^2) + 4\kappa_\sigma \left( 3y_D^2 + y_E^2 + \frac{1}{2}y_{N_3}^2 \right) - 2 \left( 3y_D^4 + y_E^4 + \frac{1}{2}y_{N_3}^4 \right), \\
16\pi^2 \mu \frac{\partial \kappa_{\sigma S}}{\partial \mu} &= 4\kappa_{\sigma S}^2 + 8(\kappa_S + \kappa_\sigma)\kappa_{\sigma S} + 2(\kappa_{\phi S}\kappa_{\phi\sigma} + \kappa_{\eta S}\kappa_{\eta\sigma}) \\
&\quad + 2\kappa_{\sigma S} \left[ 3(y_d^2 + \tilde{y}_d^2) + y_e^2 + \tilde{y}_e^2 + 3y_D^2 + y_E^2 + \frac{1}{2}y_{N_3}^2 \right] - 4[3y_D^2(y_d^2 + \tilde{y}_d^2) + y_E^2(y_e^2 + \tilde{y}_e^2)], \\
16\pi^2 \mu \frac{\partial \kappa_{\phi\sigma}}{\partial \mu} &= 4\kappa_{\phi\sigma}^2 + 2\kappa_{\sigma S}\kappa_{\phi S} + 2\kappa_{\eta\sigma}(2\lambda_3 + \lambda_4) + 4\kappa_{\phi\sigma}(3\lambda_1 + 2\kappa_\sigma) + 2\kappa_{\phi\sigma} \left( 3y_D^2 + y_E^2 + \frac{1}{2}y_{N_3}^2 + 3h_t^2 - \frac{9}{4}g^2 - \frac{3}{4}g^2 \right), \\
16\pi^2 \mu \frac{\partial \kappa_{\eta\sigma}}{\partial \mu} &= 4\kappa_{\eta\sigma}^2 + 2\kappa_{\sigma S}\kappa_{\eta S} + 2\kappa_{\phi\sigma}(2\lambda_3 + \lambda_4) + 4\kappa_{\eta\sigma}(3\lambda_2 + 2\kappa_\sigma) \\
&\quad + 2\kappa_{\eta\sigma} \left( 3y_D^2 + y_E^2 + \frac{1}{2}y_{N_3}^2 + 2h_2^2 + 3h_3^2 - \frac{9}{4}g^2 - \frac{3}{4}g^2 \right) - 4(h_2^2 + h_3^2)y_{N_3}^2, \\
16\pi^2 \mu \frac{\partial \kappa_{\phi S}}{\partial \mu} &= 4\kappa_{\phi S}^2 + 2\kappa_{\sigma S}\kappa_{\phi\sigma} + 2\kappa_{\eta S}(2\lambda_3 + \lambda_4) + 4\kappa_{\phi S}(3\lambda_1 + 2\kappa_S) + 2\kappa_{\phi S} \left[ 3(y_d^2 + \tilde{y}_d^2) + y_e^2 + \tilde{y}_e^2 + 3h_t^2 - \frac{9}{4}g^2 - \frac{3}{4}g^2 \right], \\
16\pi^2 \mu \frac{\partial \kappa_{\eta S}}{\partial \mu} &= 4\kappa_{\eta S}^2 + 2\kappa_{\sigma S}\kappa_{\eta\sigma} + 2\kappa_{\phi S}(2\lambda_3 + \lambda_4) + 4\kappa_{\eta S}(3\lambda_2 + 2\kappa_S) + 2\kappa_{\eta S} \left[ 3(y_d^2 + \tilde{y}_d^2) + y_e^2 + \tilde{y}_e^2 + 2h_2^2 + 3h_3^2 - \frac{9}{4}g^2 - \frac{3}{4}g^2 \right], \\
16\pi^2 \mu \frac{\partial y_d}{\partial \mu} &= y_d \left[ -8g_s^2 - \frac{2}{3}g^2 + \frac{1}{2}y_D^2 + 4y_d^2 + 3\tilde{y}_d^2 + y_e^2 + \tilde{y}_e^2 \right],
\end{aligned}$$

$$\begin{aligned}
16\pi^2\mu\frac{\partial\tilde{y}_d}{\partial\mu} &= \tilde{y}_d\left[-8g_s^2 - \frac{2}{3}g^2 + \frac{1}{2}y_D^2 + 3y_d^2 + 4\tilde{y}_d^2 + y_e^2 + \tilde{y}_e^2\right], \\
16\pi^2\mu\frac{\partial y_e}{\partial\mu} &= y_e\left[-6g^2 + \frac{1}{2}y_E^2 + 3(y_d^2 + \tilde{y}_d^2) + 2y_e^2 + \tilde{y}_e^2\right], \\
16\pi^2\mu\frac{\partial\tilde{y}_e}{\partial\mu} &= \tilde{y}_e\left[-6g^2 + \frac{1}{2}y_E^2 + 3(y_d^2 + \tilde{y}_d^2) + y_e^2 + 2\tilde{y}_e^2\right], \\
16\pi^2\mu\frac{\partial y_D}{\partial\mu} &= y_D\left(-8g_s^2 - \frac{2}{3}g^2 + 4y_D^2 + y_E^2 + \frac{1}{2}y_d^2 + \frac{1}{2}\tilde{y}_d^2 + \frac{1}{2}y_{N_3}^2\right), \\
16\pi^2\mu\frac{\partial y_E}{\partial\mu} &= y_E\left(-6g^2 + 3y_D^2 + 2y_E^2 + \frac{1}{2}y_e^2 + \frac{1}{2}\tilde{y}_e^2 + \frac{1}{2}y_{N_3}^2\right), \\
16\pi^2\mu\frac{\partial y_{N_3}}{\partial\mu} &= y_{N_3}\left[3y_D^2 + y_E^2 + \frac{3}{2}y_{N_3}^2 + 2(h_2^2 + h_3^2)\right], \\
16\pi^2\mu\frac{\partial h_2}{\partial\mu} &= h_2\left(-\frac{9}{4}g^2 - \frac{3}{4}g^2 + 5h_2^2 + 3h_3^2\right), \\
16\pi^2\mu\frac{\partial h_3}{\partial\mu} &= h_3\left(-\frac{9}{4}g^2 - \frac{3}{4}g^2 + 2h_2^2 + \frac{15}{2}h_3^2 + \frac{1}{2}y_{N_3}^2\right), \\
16\pi^2\mu\frac{\partial h_t}{\partial\mu} &= h_t\left(\frac{9}{2}h_t^2 - 8g_s^2 - \frac{9}{4}g^2 - \frac{17}{12}g^2\right), \\
16\pi^2\mu\frac{\partial g_s}{\partial\mu} &= -\frac{19}{3}g_s^3, \\
16\pi^2\mu\frac{\partial g}{\partial\mu} &= -3g^3, \\
16\pi^2\mu\frac{\partial g'}{\partial\mu} &= \frac{79}{9}g'^3,
\end{aligned} \tag{B1}$$

where  $g_s$ ,  $g$ , and  $g'$  are the gauge coupling constants of the SM. In these equations, we assume Eq. (20) for neutrino Yukawa couplings and Eq. (A1) for  $y_f$  and  $\tilde{y}_f$ , and also only  $y_{N_3}$  is taken into account. Contributions from  $V_b$  are also neglected in these RGEs.

Initial values of the coupling constants which are used in the RGE study of the right panel of Fig. 1 are taken to be the same ones that are used in the analysis of the leptogenesis for the case (I). A part of them are fixed at the weak scale as

$$\begin{aligned}
\tilde{\lambda}_1 &= 0.13, & \tilde{\lambda}_2 &= 0.1, & \tilde{\lambda}_3 &= 0.445, & \lambda_4 &= -0.545, & \lambda_5 &= -10^{-3}, \\
h_1 &= 6 \times 10^{-7}, & h_2 &= 8.3 \times 10^{-3}, & h_3 &= 3.9 \times 10^{-3},
\end{aligned} \tag{B2}$$

where  $\tilde{\lambda}_3$  and  $\lambda_4$  are fixed by the DM constraint shown in the left panel of Fig. 1 and  $h_{2,3}$  are fixed by using the neutrino mass formula and the neutrino oscillation data. Remaining ones are fixed at a scale  $\bar{M}$  as

$$\begin{aligned}
\tilde{\kappa}_S &= 10^{-8}, & \tilde{\kappa}_\sigma &= 10^{-4.5}, & |\kappa_{\sigma S}| &= 10^{-6.1}, & \kappa_{\phi\sigma} &= \kappa_{\eta\sigma} = 10^{-4}, & \kappa_{\phi S} &= \kappa_{\eta S} = 10^{-7} \\
y_{N_1} &= 7 \times 10^{-3}, & y_{N_2} &= 2 \times 10^{-2}, & y_{N_3} &= 4 \times 10^{-2}, \\
y_D &= y_E = 10^{-1.2}, & y_e &= y_d = 8 \times 10^{-4}, & \tilde{y}_e &= \tilde{y}_d = 4 \times 10^{-4}.
\end{aligned} \tag{B3}$$

These satisfy the imposed conditions (5), (14), (17), (31), and (39).

- [1] M. Kobayashi and T. Maskawa, *Prog. Theor. Phys.* **49**, 652 (1973).
- [2] R. Jackiw and C. Rebbi, *Phys. Rev. Lett.* **37**, 172 (1976); C. G. Callan, R. F. Dashen, and D. J. Gross, *Phys. Lett.* **63B**, 334 (1976).
- [3] P. A. Zyla *et al.* (Particle Data Group), *Prog. Theor. Exp. Phys.* **2020**, 083C01 (2020).
- [4] I. S. Altarev *et al.*, *Nucl. Phys.* **A341**, 269 (1980).
- [5] For reviews J. E. Kim, *Phys. Rep.* **150**, 1 (1987); J. E. Kim and G. Carosi, *Rev. Mod. Phys.* **82**, 557 (2010).
- [6] R. D. Peccei and H. R. Quinn, *Phys. Rev. Lett.* **38**, 1440 (1977); *Phys. Rev. D* **16**, 1791 (1977).
- [7] E. Witten, *Nucl. Phys.* **B258**, 75 (1985); S. Kalara and R. N. Mohapatra, *Phys. Rev. D* **35**, 3143 (1987); M. Matsuda, T. Matsuoka, H. Mino, D. Suematsu, and Y. Yamada, *Prog. Theor. Phys.* **79**, 174 (1988); D. Suematsu, *Phys. Rev. D* **38**, 3128 (1988).
- [8] A. Nelson, *Phys. Lett.* **136B**, 387 (1984); S. M. Barr, *Phys. Rev. Lett.* **53**, 329 (1984); A. Nelson, *Phys. Lett.* **143B**, 165 (1984).
- [9] M. Dine and P. Draper, *J. High Energy Phys.* **08** (2015) 132.
- [10] L. Bento, G. C. Branco, and P. A. Parada, *Phys. Lett. B* **267**, 95 (1991).
- [11] D. Suematsu, *Phys. Rev. D* **100**, 055019 (2019); *Eur. Phys. J. C* **81**, 311 (2021).
- [12] B. Pontecorvo, *Sov. Phys. JETP* **6**, 429 (1957); **7**, 172 (1958); Z. Maki, M. Nakagawa, and S. Sakata, *Prog. Theor. Phys.* **28**, 870 (1962).
- [13] M. A. Acero *et al.* (NovA Collaboration), *Phys. Rev. Lett.* **123**, 151803 (2019); K. Abe *et al.* (The T2K Collaboration), *Nature (London)* **580**, 339 (2020).
- [14] P. A. R. Ade *et al.* (Planck Collaboration), *Astron. Astrophys.* **571**, A22 (2014); P. A. R. Ade *et al.* (BICEP2/Keck and Planck Collaborations), *Phys. Rev. Lett.* **114**, 101301 (2015); P. A. R. Ade *et al.* (Planck Collaboration), *Astron. Astrophys.* **594**, A20 (2016).
- [15] N. Aghanim *et al.* (Planck Collaboration), *Astron. Astrophys.* **641**, A6 (2020).
- [16] For reviews, D. H. Lyth and A. Riotto, *Phys. Rep.* **314**, 1 (1999); A. R. Liddle and D. H. Lyth, *Cosmological Inflation and Large-Scale Structure* (Cambridge University Press, Cambridge, England, 2000).
- [17] F. L. Bezrukov and M. Shaposhnikov, *Phys. Lett. B* **659**, 703 (2008); F. L. Bezrukov, A. Magnin, and M. Shaposhnikov, *Phys. Lett. B* **675**, 88 (2009).
- [18] B. L. Spokoiny, *Phys. Lett. B* **147**, 39 (1984); D. S. Salopek, J. R. Bond, and J. M. Bardeen, *Phys. Rev. D* **40**, 1753 (1989).
- [19] G. Degrassi, S. Di Vita, J. Elias-Miro, J. R. Espinoza, G. F. Giudice, G. Isidori, and A. Strumia, *J. High Energy Phys.* **08** (2012) 098; D. Buttazzo, G. Degrassi, P. P. Giardino, G. F. Giudice, F. Sala, A. Salvio, and A. Strumia, *J. High Energy Phys.* **12** (2013) 089; F. Bezrukov, M. Y. Kalmykov, B. A. Kniehl, and M. Shaposhnikov, *J. High Energy Phys.* **10** (2012) 140; S. Alekhin, A. Djouadi, and S. Moch, *Phys. Lett. B* **716**, 214 (2012); A. V. Bednyakov, B. A. Kniehl, A. F. Pikelner, and O. L. Veretin, *Phys. Rev. Lett.* **115**, 201802 (2015).
- [20] J. L. F. Barb3n and J. R. Espinosa, *Phys. Rev. D* **79**, 081302 (R) (2009); C. P. Burgess, H. M. Lee, and M. Trott, *J. High Energy Phys.* **07** (2010) 007; M. P. Hertzberg, *J. High Energy Phys.* **11** (2010) 023; D. I. Kaiser, *Phys. Rev. D* **81**, 084044 (2010); R. N. Lerner and J. McDonald, *J. Cosmol. Astropart. Phys.* **11** (2012) 019.
- [21] Y. Ema, R. Jinno, K. Mukaida, and K. Nakayama, *J. Cosmol. Astropart. Phys.* **02** (2017) 045.
- [22] D. Suematsu, *Eur. Phys. J. C* **78**, 33 (2018).
- [23] J. E. Kim, *Phys. Rev. Lett.* **43**, 103 (1979); M. A. Shifman, A. I. Vainshtein, and V. I. Zakharov, *Nucl. Phys.* **B166**, 493 (1980).
- [24] P. Sikivie, *Phys. Rev. Lett.* **48**, 1156 (1982).
- [25] A. Vilenkin and A. E. Everett, *Phys. Rev. Lett.* **48**, 1867 (1982).
- [26] H. E. Haber and Z. Surujon, *Phys. Rev. D* **86**, 075007 (2012).
- [27] J. Preskill, M. B. Wise, and F. Wilczek, *Phys. Lett.* **120B**, 127 (1983); L. F. Abbott and P. Sikivie, *Phys. Lett.* **120B**, 133 (1983); M. Dine and W. Fischler, *Phys. Lett.* **120B**, 137 (1983).
- [28] S. Weinberg, *Phys. Rev. Lett.* **40**, 223 (1978); F. Wilczek, *Phys. Rev. Lett.* **40**, 279 (1978).
- [29] L. Di Luzio, F. Mescia, and E. Nardi, *Phys. Rev. D* **96**, 075003 (2017).
- [30] E. Ma, *Phys. Rev. D* **73**, 077301 (2006).
- [31] J. Kubo, E. Ma, and D. Suematsu, *Phys. Lett. B* **642**, 18 (2006); J. Kubo and D. Suematsu, *Phys. Lett. B* **643**, 336 (2006); E. Ma, *Ann. Fond. Louis de Broglie* **31**, 285 (2006); D. A. Sierra, J. Kubo, D. Suematsu, D. Restrepo, and O. Zapata, *Phys. Rev. D* **79**, 013011 (2009); D. Suematsu, T. Toma, and T. Yoshida, *Phys. Rev. D* **82**, 013012 (2010); H. Fukuoka, J. Kubo, and D. Suematsu, *Phys. Lett. B* **678**, 401 (2009); D. Suematsu and T. Toma, *Nucl. Phys.* **B847**, 567 (2011); H. Fukuoka, D. Suematsu, and T. Toma, *J. Cosmol. Astropart. Phys.* **07** (2011) 001.
- [32] S. Kashiwase and D. Suematsu, *Phys. Rev. D* **86**, 053001 (2012); *Eur. Phys. J. C* **73**, 2484 (2013).
- [33] T. Hashimoto and D. Suematsu, *Phys. Rev. D* **102**, 115041 (2020).
- [34] E. Aprile *et al.* (XENON Collaboration), *Phys. Rev. Lett.* **121**, 111302 (2018).
- [35] D. Suematsu, T. Toma, and T. Yoshida, *Phys. Rev. D* **79**, 093004 (2009).
- [36] R. N. Lerner and J. McDonald, *Phys. Rev. D* **80**, 123507 (2009); **83**, 123522 (2011).
- [37] D. Suematsu, *Phys. Rev. D* **85**, 073008 (2012); *Phys. Lett. B* **760**, 538 (2016); R. H. S. Budhi, S. Kashiwase, and D. Suematsu, *Phys. Rev. D* **90**, 113013 (2014); *J. Cosmol. Astropart. Phys.* **09** (2015) 039; *Phys. Rev. D* **93**, 013022 (2016); S. Kashiwase and D. Suematsu, *Phys. Lett. B* **749**, 603 (2015).
- [38] G. Ballesteros, J. Redondo, A. Ringwald, and C. Tamarit, *J. Cosmol. Astropart. Phys.* **08** (2017) 001.
- [39] P. B. Greene, L. Kofman, A. Linde, and A. A. Starobinsky, *Phys. Rev. D* **56**, 6175 (1997).
- [40] L. Kofman, A. Linde, and A. A. Starobinsky, *Phys. Rev. D* **56**, 3258 (1997).
- [41] I. Tkachev, S. Khlebnikov, L. Kofman, and A. Linde, *Phys. Lett. B* **440**, 262 (1998).
- [42] G. Felder, L. Kofman, and A. Linde, *Phys. Rev. D* **59**, 123523 (1999).

- [43] A. Riotto and M. Trodden, *Annu. Rev. Nucl. Part. Sci.* **49**, 35 (1999); W. Bernreuther, *Lect. Notes Phys.* **591**, 237 (2002); M. Dine and A. Kusenko, *Rev. Mod. Phys.* **76**, 1 (2003).
- [44] M. Fukugita and T. Yanagida, *Phys. Lett. B* **174**, 45 (1986); W. Buchmüller, P. Di Bari, and M. Plümacher, *Ann. Phys. (Amsterdam)* **315**, 305 (2005).
- [45] S. Davidson and A. Ibarra, *Phys. Lett. B* **535**, 25 (2002).
- [46] T. Hogle, M. Platscher, and K. Schmitz, *Phys. Rev. D* **98**, 023020 (2018).
- [47] D. Suematsu, *Phys. Rev. D* **100**, 055008 (2019).
- [48] L. L. Honorez, E. Nerzi, J. F. Oliver, and M. H. G. Tytgat, *J. Cosmol. Astropart. Phys.* **02** (2007) 028; T. Hambye, F.-S. Ling, L. L. Honorez, and J. Roche, *J. High Energy Phys.* **07** (2009) 090.
- [49] S. Andreas, M. H. G. Tytgat, and Q. Swillens, *J. Cosmol. Astropart. Phys.* **04** (2009) 004.
- [50] For reviews P. Sikivie, *Lect. Notes Phys.* **741**, 19 (2008); D. J. E. Marsh, *Phys. Rep.* **643**, 1 (2016).
- [51] M. Beltrán, J. García-Bellido, and J. Lesgourgues, *Phys. Rev. D* **75**, 103507 (2007); M. P. Hertzberg, M. Tegmark, and F. Wilczek, *Phys. Rev. D* **78**, 083507 (2008).
- [52] M. Fairbairn, R. Hogan, and D. J. E. Marsh, *Phys. Rev. D* **91**, 023509 (2015).
- [53] D. J. E. Marsh, *Phys. Rep.* **643**, 1 (2016).
- [54] C. Jarlskog, *Phys. Rev. Lett.* **55**, 1039 (1985).